Annu. Rev. Astron. Astrophys. 1995. 33:581–624

INWARD BOUND—THE SEARCH FOR SUPERMASSIVE BLACK HOLES IN GALACTIC NUCLEI

John Kormendy[1]

Institute for Astronomy, University of Hawaii, 2680 Woodlawn Drive, Honolulu, Hawaii 96822

Douglas Richstone

Department of Astronomy, University of Michigan, Dennison Building, Ann Arbor, Michigan 48109

KEY WORDS: dead quasars, galactic dynamics, galactic nuclear activity

ABSTRACT

Dynamical searches reveal central dark objects with masses $\sim 10^6$ to $10^{9.5} M_\odot$ in the Galaxy, M31, M32, M87, NGC 3115, NGC 3377, NGC 4258, and NGC 4594. Indirect arguments suggest but do not prove that these are supermassive black holes (BHs) like those postulated as quasar engines. This paper reviews dynamical search techniques, the robustness of the evidence, and BH demographics. Stellar-dynamical evidence is generally more robust than gas-dynamical evidence (gas velocities can be nongravitational), but gas measurements reach closer to the Schwarzschild radius, and in NGC 4258 they show a Keplerian rotation curve. A statistical survey finds BHs in ~20% of nearby E–Sbc galaxies, consistent with predictions based on quasar energetics. BH masses are proportional to the mass of the bulge component. Most candidates are inactive; in some cases, the abundance of fuel is not easily reconciled with BH starvation. Flashes caused by the accretion of individual stars may provide a test of the BH picture.

[1]Visiting Astronomer, Canada-France-Hawaii Telescope (CFHT), operated by the National Research Council of Canada, le Centre National de la Recherche Scientifique of France, and the University of Hawaii.

0066–4146/95/0915-0581$05.00

1. INTRODUCTION

The idea that active galactic nuclei (AGNs) are powered by accretion onto supermassive black holes (BHs) is based on compelling theoretical arguments (Salpeter 1964; Zel'dovich 1964; Lynden-Bell 1969, 1978; Lynden-Bell & Rees 1971; see Rees 1984; Begelman et al 1984; Blandford 1990; and Blandford & Rees 1992 for reviews), a broad array of circumstantial evidence, and a few incisive observations. The latter include rapid time variability and superluminal jets, which suggest that AGN engines are relativistically compact. Theory predicts BH masses of 10^6–$10^{9.5} M_\odot$. But the BH mass function and the distribution of BHs among galaxies depend on AGN lifetimes and are poorly constrained. This much is clear: Quasars were overwhelmingly more numerous at $z \gtrsim 2$ than they are now, so dead quasar engines should be hiding in many nearby galaxies.

The weak spot in this picture is the lack of proof that BH engines exist. This motivates many searches. But a great deal is at stake. The BH picture has become our paradigm. This situation is dangerous: It is easy to believe that we have proved what we expect to find.

This paper reviews stellar- and gas-dynamical evidence for black holes (complete through December 1994). Previous reviews are given by Sargent (1987), Richstone (1988, 1993), Filippenko (1988), Dressler (1989), Davies (1989), Gerhard (1992), Kormendy (1992a,b, 1993, 1994), de Zeeuw (1994), and van der Marel (1994c). Gas is very responsive to nongravitational forces, so the most definitive searches are based on stellar kinematics. Section 2 summarizes the state of the search and lists the eight detections. Section 3 shows why cuspy brightness profiles are not evidence for black holes. After a summary of search techniques, Section 4 discusses the stellar-dynamical BH candidates. An important upper limit is discussed in Section 4.8. Section 5 discusses the detections based on gas dynamics. A preliminary review of BH demographics is given in Section 6. Section 7 considers whether the detected candidates are too inactive to be BHs. Conclusions and a wish list are given in Section 8.

The case is now strong that 10^6- to $10^{9.5}$-$M_\odot$ dark objects have been discovered in a few galaxies. All are objects in which the search is relatively easy because circumstances are favorable (e.g. the center rotates rapidly). In most galaxies, we do not even have limits; when they are available, they are weak. This especially includes the giant ellipticals that motivated the search because of AGN activity. Despite the difficulty of BH detection, the amount of nuclear dark matter is consistent with theoretical predictions. But the rigor stops here. Suggestions that the dark objects are BHs are based only on indirect astrophysical arguments.

What we need next is a significant iteration in the quality of the data. We need to see whether the BH case gets stronger or weaker as the spatial resolution and modeling techniques improve. We also need better constraints on the radius

inside which the dark mass lies to confirm or exclude alternatives to BHs. Improved ground-based instruments and especially the *Hubble Space Telescope* (*HST*) are beginning to provide this iteration. Early results are encouraging. But the case is not ready to go to the jury. By themselves, neither the dynamics nor the AGN observations are conclusive. Together, they make a compelling picture.

Our title does homage to A Pais's (1986) book *Inward Bound*, an elegant history of twentieth-century physics as it probed to smaller and smaller subatomic length scales. The BH search is similarly a journey. We make incremental improvements in spatial resolution, each expensive in ingenuity and money. This paper reviews the first order of magnitude of the inward journey in radius. But we are still observing at 10^5 Schwarzschild radii. Surprises are possible on the way to the center.

2. PRESENT STATUS OF THE BLACK HOLE SEARCH

The search can be divided into three parts:

1. Look for dynamical evidence of central dark masses. In practice, we look for high mass-to-light ratios. If M/L increases toward the center to values that are several times larger than normal, this is a meaningful clue because the range of M/L values in old stellar populations is small. Is there any escape from the conclusion that M/L is high? If not, then we have discovered a "massive dark object" (MDO). It could be a supermassive black hole, it could be a cluster of low-mass stars, brown dwarfs, or stellar remnants, or it could be halo dark matter.

2. Once a few MDOs have been found, we need to improve the observations enough so that alternatives to a BH can be confirmed or ruled out. Proof of a BH requires detection of relativistic velocities in orbits at a few Schwarzschild radii. This is not imminent. But in practice, the most plausible alternative to a BH is a cluster of stellar remnants; it would already be important progress if we could rule out such a cluster on physical grounds. When we say that "we have evidence for a BH" in some galaxy, we mean we find such arguments persuasive. When we say "we have found an MDO," we are emphasizing the uncertainty in arguments against BH alternatives. Step 2 of the BH search is just beginning; we will say little about it here.

3. Black hole astrophysics requires more than the detection of a few examples. Ultimately, we want to know the mass function and frequency of incidence of BHs in various types of galaxies. This requires statistical surveys. Surveys are challenging because BH detectability depends on galaxy type. For example, BH detection is easier in rotating disk galaxies than in nonrotating giant ellipticals. Type-dependent biases will be a problem. In practice, we

make statistical surveys in parallel with step 2. If MDOs turn out not to be BHs, the demographic results will nevertheless be important to our understanding of galaxy nuclei and AGN activity. BH surveys are reviewed in Section 6.

At present, we are nearing the end of step 1. We have dynamical evidence for massive dark objects in eight galaxies. Table 1 lists them subjectively in order from most secure to most weak, separately for detections based on stellar and gas dynamics.

But step 1 is not quite finished. For all objects, the MDO discovery observations have been confirmed by at least one other group. Some of these papers improve significantly on the analysis. But none improves much on the discovery resolution. The next iteration in the search—a substantial improvement in spatial resolution—is in progress.

Most of this paper is a review of step 1. How robust is the claim that MDOs have been detected? What kind of evidence should we believe?

3. CUSPY DENSITY PROFILES ARE NOT EVIDENCE FOR BLACK HOLES

Many papers argue that the brightness profiles of particular galaxies imply that they contain BHs (e.g. Young et al 1978, 1979; Lauer et al 1991a, 1992a,b; Fabbiano et al 1994). The arguments are variations on the theme that BHs produce cuspy potentials and hence cuspy density distributions. This section shows why such arguments are inconclusive.

Figure 1 shows projected brightness profiles of six stellar systems. Identifications are omitted. Which objects show evidence for a BH? Are they the ones with high central densities or small core radii?

The answers are in Figure 2. M31 and M32 show stellar-dynamical evidence for high central mass-to-light ratios. Deconvolved *HST* profiles are shown for both galaxies. To be sure, they are very compact. But M33's nucleus (Kormendy & McClure 1993) is more compact than that of M31. It is as small as the limit on a core in M32, and it is almost as dense. And yet we know that M33 does not contain a supermassive BH. Kormendy & McClure (1993) find that the central velocity dispersion is only $\sigma = 21 \pm 3$ km s^{-1}. Therefore, $M_\bullet \lesssim 5 \times 10^4 M_\odot$ (Section 4.8).

In contrast, M87 contains an MDO of mass $M_\bullet \sim 3 \times 10^9 M_\odot$ (Sargent et al 1978, Harms et al 1994). But its highest measured surface brightness is more than 50 times lower than that of the M33 nucleus, and its core is more than 1000 times larger. At radii $r \lesssim GM_\bullet/\sigma^2 \simeq 1''$ that are dominated by the BH (Wolfe & Burbidge 1970, Peebles 1972, Bahcall & Wolf 1976), M87 does not even reach the surface brightnesses seen in normal ellipticals like NGC 3379, in which there is no evidence (circumstantial or otherwise) for a BH.

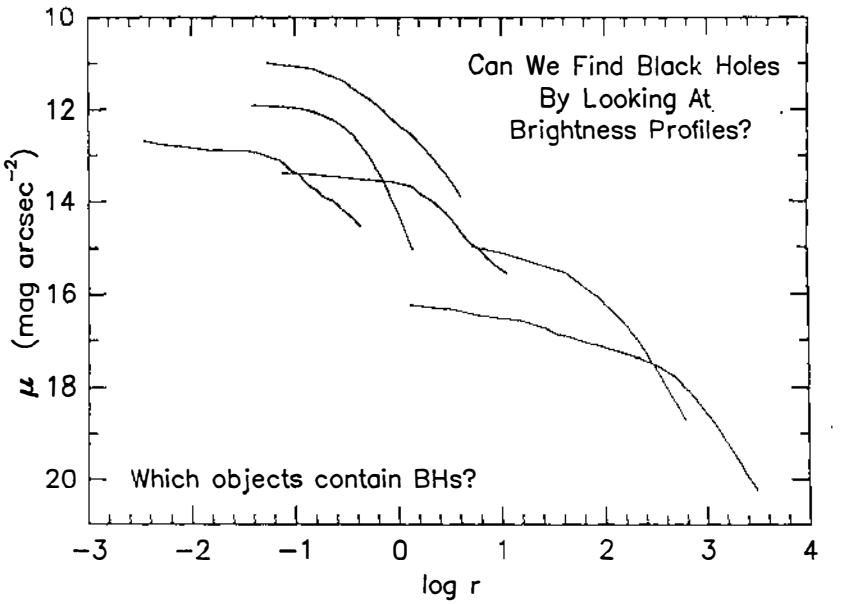

Figure 1 Seeing-corrected, mean brightness profiles of six stellar systems. Can you identify the ones that contain supermassive BHs?

Finally, the core-collapsed globular cluster M15 (Lauer et al 1991b) has a smaller core radius than any galactic nucleus. Its central density is much higher than that of M87. But it shows no evidence for a BH. From Newell et al (1976), Peterson et al (1989), Meylan & Pryor (1993), Dubath et al (1994), and Dubath & Meylan (1994), we adopt $M_\bullet < 10^3\, M_\odot$.

To emphasize this further, Figure 3 shows BH mass vs core parameters as measured with *HST* (Kormendy et al 1994, Lauer et al 1995, Faber et al 1995). *The correlations are opposite to what we expect.* Far from making cores compact, *larger BH masses are associated with larger cores and lower maximum densities.* These correlations may be upper envelopes of a distribution: only two upper limits are plotted.

The explanation of Figure 3 becomes clear when we plot $M_\bullet$ against bulge luminosity (Figure 14 in Section 6). There is a good correlation: More massive BHs are found in more luminous bulges. But we know that more luminous bulges have larger $r_b \simeq r_c$ and fainter μ_{0V}: These are projections of the fundamental plane correlations (see Kormendy & Djorgovski 1989 for a review). Therefore, at 0.″1 resolution, it is the virial theorem controlling the formation of the whole galaxy (Faber et al 1987, Djorgovski et al 1988) and not $M_\bullet$ that determines the compactness of the core. BH cusps may dominate over the fundamental plane correlations at still smaller radii, but we will need better resolution to see this.

Table 1 MDO census

Galaxy	Type[a]	D [b] (Mpc)	$M_{B,\rm bulge}$ [c]	$F_{\rm radio}$ [d] (mJy)	$\frac{L_{\rm radio}}{L_{\rm radio}(\rm SgrA^*)}$ [e]	$M_\bullet$ [f] ($M_\odot$)	$\log\frac{M_\bullet}{M_{\rm bulge}}$ [g]	References[h]
M31	Sb	0.7	−18.82	0.03	0.3	3×10^7	−3.31	Dressler & Richstone 88; Kormendy 88c; Richstone+90 (also M32); Bacon+94
NGC 3115	S0/	8.4	−19.90	<0.33	<460.	1×10^9	−1.92	Kormendy & Richstone 92
M32	E	0.7	−15.51	<4.	<54.	2×10^6	−2.60	Tonry 84, 87; Dressler & Richstone 88; van der Marel+94b; Qian+95; Dehnen 95
NGC 4594	Sa/	9.2	−21.21	$\sim10^2$	$\sim2\times10^5$	5×10^8	−2.99	Kormendy 88d; Emsellem+94a
Galaxy	Sbc	0.0085	−17.65	7×10^2	1.	2×10^6	−3.78	McGinn+89; Sellgren+90; Kent 92; Genzelt 94a; Evans & de Zeeuw 94; Haller+95; Krabbe+95
NGC 3377	E	9.9	−18.80	<0.5	$<1\times10^3$	8×10^7	−2.24	Kormendy+95b
NC 4258	Sbc	7.5	−17.3	1.8	2×10^3	4×10^7	−2.05	Miyoshi+95
M87	E	15.3	−21.42	$\sim10^3$	$\sim7\times10^6$	3×10^9	−2.32	Sargent+78; Harms+94; van der Marel 94a

[a] Morphological type (de Vaucouleurs & Pence 1978, de Vaucouleurs et al 1991).

[b] Distance (mostly Faber et al 1995; for NGC 4258: S Faber 1995, personal communication). Values are only slightly modified from those of Lynden-Bell et al (1988) and Faber et al (1989). They are based on a large-scale flow field solution, an assumed Virgo Cluster distance of 15.3 Mpc, and a Hubble constant of $H_0 = 80$ km s^{-1} Mpc^{-1}. They agree well with distances in Tully et al (1992). BH mass scales as D; $\log M_\bullet/M_{\rm bulge}$ is independent of D. Demographic conclusions are not sensitive to the distance scale: see versions of Figures 1, 2, 3, and 14 for $H_0 = 50$ km s^{-1} Mpc^{-1} in Kormendy (1993, 1994).

[c] B-band bulge absolute magnitude, based mostly on B_T in de Vaucouleurs et al (1991). Exceptions are M31 ($V_T = 3.28$ from Kent 1987b), NGC 3115 ($B_T = 9.75$ from Capaccioli et al 1987), NGC 4594 ($B_T = 8.65$ from Burkhead 1986), and the Galaxy (M_B adapted from Kent et al 1991). Galactic absorptions are taken from Burstein & Heiles (1984). Assumed bulge-to-total luminosity ratios are: $B/T = 0.24$ in M31 (de Vaucouleurs 1958), 0.94 in NGC 3115 (Capaccioli et al 1987), 0.93 in NGC 4594 (Burkhead 1986), and 0.063 in NGC 4258 (an approximate value near the bottom of the *distribution* of B/T values for Sbc galaxies; see Simien & de Vaucouleurs 1986).

[d] Nuclear radio continuum flux. Wavelengths and sources—M31: 3.6 cm, Crane et al (1992, 1993a); NGC 3115: 6 cm, Fabbiano et al (1989); M32: 21 cm, Hummel (1980); NGC 4594: 3.6–21 cm, van der Kruit (1973), de Bruyn et al (1976), Hummel (1980); the Galaxy: 6 cm, Zhao et al (1992); NGC 3377: 6 cm, Wrobel & Heeschen (1991); NGC 4258: 6 cm, Turner & Ho (1994); M87: 2 cm, 21 cm, Hummel (1980), Biretta et al (1983). The value for M87 depends on how much of the jet is included at the spatial resolution of the observations.

[e] Nuclear radio luminosity in units of the luminosity of Sgr A* at the same wavelength. Sgr A* fluxes are 0.5, 0.7, 0.8, and 0.9 Jy at 21 cm, 6 cm, 3.6 cm, and 2 cm, respectively (Zhao et al 1992).

[f] MDO mass for the best-fitting isotropic dynamical model.

[g] Logarithm of MDO mass fraction; $M_{\rm bulge}$ is the bulge mass determined from $M_{B,\rm bulge}$ and from M/L ratios measured in the BH papers (see note h). For NGC 4258, $M/L_r = 4.08$ is from Kent (1987a); this disk value is probably a good approximation for the bulgelike component as well.

[h] MDO references; et al *is abbreviated as* + and (e.g.) 1994 as 94. Only papers that measured $M_\bullet$ are included; additional papers that confirm the kinematics are discussed in Sections 4 and 5.

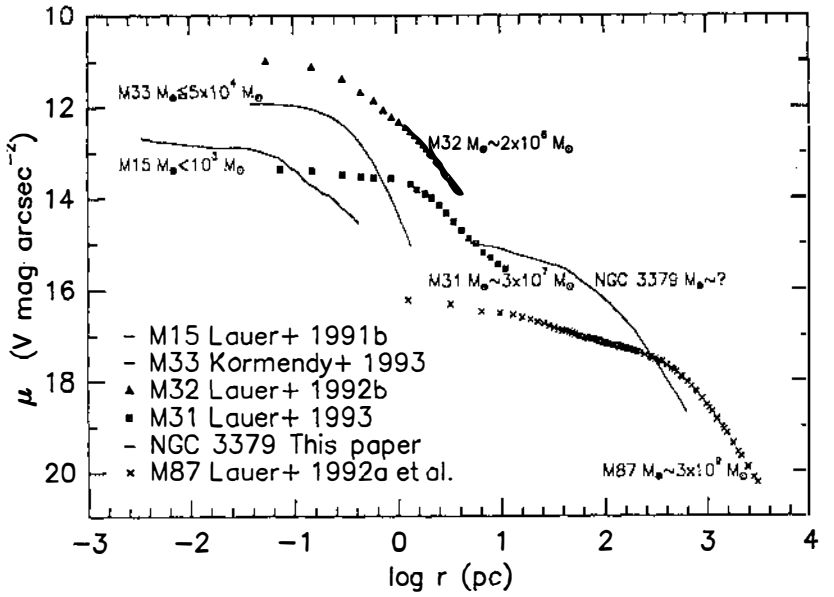

Figure 2 Figure 1 with object names and BH masses identified.

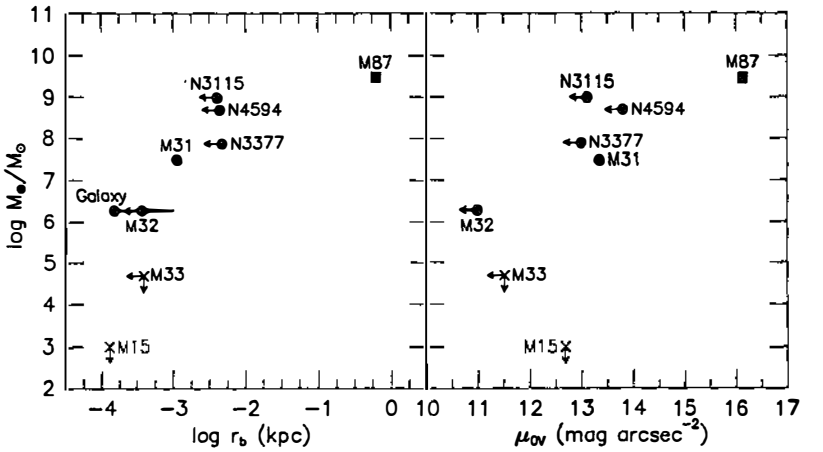

Figure 3 BH mass as a function of profile break radius r_b (formerly core radius r_c) and maximum observed surface brightness μ_{0V} (cf figure 4 in Kormendy 1994). *HST* measurements of r_b and μ_{0V} are from Faber et al (1995). Filled circles and squares show objects with stellar- and gas-dynamical evidence for MDOs. Upper limits on $M_\bullet$ are plotted as crosses. Strong limits on core parameters are indicated by arrows. For the Galaxy, r_b is from r_c as given in Allen (1994), Eckart et al (1994), Genzel et al (1994b), and Rieke & Rieke (1994); the horizontal error bar ends at the larger of two values quoted by Rieke & Rieke and by Allen.

We conclude that evidence for black holes based only on surface brightness profiles is not evidence at all (see also Phinney 1989). This includes arguments like: (*a*) the profile is cuspy; (*b*) central densities are high and core radii are small; or (*c*) the central relaxation time is short, so core collapse is likely. These arguments apply most strongly to M33, and in M33 a supermassive BH can be excluded. Unless kinematic measurements prove that mass-to-light ratios rise to large values near the center, high central densities are most likely to be evidence for dissipation (Phinney 1989, Kormendy 1989). Dissipation can produce arbitrarily high densities. Witness planets.

4. STELLAR-DYNAMICAL BLACK HOLE SEARCHES

Sections 4 and 5 review stellar- and gas-dynamical BH searches. Detections are listed in Table 1. Except for M33 (Section 4.8), we do not discuss $M_\bullet$ upper limits; these can be found in Bower et al (1993) and in van den Bosch & van der Marel (1995).

This subject began with two papers on the stellar dynamics of M87 (Young et al 1978, Sargent et al 1978). They showed that M87 contains an $M_\bullet \simeq 3 \times 10^9$ $M_\odot$ MDO if the stellar velocity distribution is isotropic. We now know that isotropy is unlikely, but these papers nevertheless were seminal. Recently, Harms et al (1994) have confirmed the conclusions of Sargent, Young, and collaborators using the refurbished *HST*. This work is based on emission-line spectroscopy, so we discuss it in Section 5.

4.1 *Search Technique*

Dynamical mass measurements are conceptually simple. We need to deal with projection and atmospheric blurring ("seeing"); this is time-consuming, but it is routine. Mainly, the analysis is complicated because we need to be careful. This subject is dangerous. We enter it with expectations. We need to protect ourselves, lest we convince ourselves prematurely that we have proved what we expect to find.

The search technique is best described in the idealized case of spherical symmetry and a velocity ellipsoid that everywhere points at the center. The first velocity moment of the collisionless Boltzmann equation gives the mass $M(r)$ within radius r,

$$M(r) = \frac{V^2 r}{G} + \frac{\sigma_r^2 r}{G}\left[-\frac{d\ln \nu}{d\ln r} - \frac{d\ln \sigma_r^2}{d\ln r} - \left(1 - \frac{\sigma_\theta^2}{\sigma_r^2}\right) - \left(1 - \frac{\sigma_\phi^2}{\sigma_r^2}\right)\right], \quad (1)$$

where V is the rotation velocity; σ_r, σ_θ, and σ_ϕ are the radial and azimuthal components of the velocity dispersion; and G is the gravitational constant. The density ν is not the total mass density ρ; it is the density of the tracer population whose kinematics we measure. We never see ρ, because the stars that contribute most of the light contribute almost none of the mass. In practice,

calculations are made assuming $\nu(r) \propto$ volume brightness, i.e. we assume that M/L for the tracer population is independent of radius. This can be (but usually is not) checked using measurements of color or line-strength gradients.

All quantities in Equation 1 are unprojected. We observe projected brightnesses, velocities, and velocity dispersions, so we must derive the ranges of unprojected quantities that are consistent with the observations after projection and seeing convolution. This is tricky. .

Kormendy (1988a,c,d) and Dressler & Richstone (1988) independently developed a method of deriving unprojected velocities from the data. Beginning with a trial set of unprojected kinematics, they first calculate model spectra projected along each line of sight by adding spectra of appropriate V and σ weighted by the local volume brightness. They then convolve the two-dimensional array of projected spectra with the point-spread function. Finally, they "observe" the model with their velocity calculator and iterate it until it agrees with the data. Further, Kormendy does not try to prove uniqueness; rather, he constructs fits that bracket the observations in surface brightness $I(r)$ and in projected $V(r)$ and $\sigma(r)$. In particular, he derives low-mass "error bar" models in which V and σ are too small near the center. The above procedure is required because of the complicated response of any velocity calculator to population mixes and to rotational line broadening. It guarantees that non-Gaussian line-of-sight velocity distributions (LOSVDs) are measured in the same way in the galaxies and models. (It does not guarantee that the models have the same LOSVDs as the galaxies; more about this is presented shortly.) If the implied M/L rises rapidly as $r \rightarrow 0$, then we have found an MDO.

Some general properties of the mass measurements follow directly from Equation 1. Rotation and random motions contribute similarly to $M(r)$, but the $\sigma^2 r/G$ term is multiplied by a factor that involves uncertainties and that can be less than 1. Thus, rapid rotation is a more secure indicator of large masses than are large velocity dispersions. Second, Equation 1 shows why velocity anisotropy is so important, especially in nonrotating giant ellipticals. *HST* data show that these have shallow power-law profiles $I \propto r^{-0.1\pm0.1}$ at $r \ll r_b$ (Lauer et al 1992a, Crane et al 1993b, Stiavelli et al 1993, Kormendy et al 1994, Forbes 1994, Forbes et al 1994, Ferrarese et al 1994, Lauer et al 1995). Then $-d\ln\nu/d\ln r \lesssim +1$. The second term cannot be larger than $+1$. But the third and fourth terms are negative if σ_r is larger than σ_θ and σ_ϕ. They can be as small as -1 each, so they can largely cancel the first two terms. This does not prove that anisotropic models are realistic, but it does illustrate why they have been so successful in explaining the kinematics of giant ellipticals without BHs (e.g. M87: Section 5.1). In contrast, a BH case is more secure if the density gradient is steep, other things being equal. This is one reason why low-luminosity ellipticals like M32 (Section 4.4) and NGC

3377 (Section 4.7) are better BH candidates than giant ellipticals: No core is resolved, so $-d \ln \nu / d \ln r \gtrsim +2$ in Equation 1.

Velocity anisotropy has usually been explored by constructing maximum entropy dynamical models (Richstone & Tremaine 1984, 1988). Once anisotropy becomes the default assumption, it is inherently difficult to prove that an MDO is required: The parameter space to be explored is large, and nature knows more distribution functions than we do. Therefore, the biggest advantage of the maximum entropy modeling technique is that it can easily be instructed to find the most extreme possible models in the most relevant directions in parameter space. In particular, it can be instructed to minimize the central mass (it does so by maximizing the anisotropy). If this fails—if M/L still rises toward the center—then we can be almost certain that an MDO is present.

We say "almost" because published maximum entropy models have had significant limitations. Flattening corrections were made post hoc using the tensor virial theorem. Also, the velocity dispersion σ_ϕ in the rotation direction was not completely free: $\sigma_\phi^2 + V^2 = \sigma_\theta^2$. This means, for example, that it was never possible to make *isotropic* models that rotate. Both limitations will be lifted in future papers. Like other analyses in astronomy, the above procedures provide results at some level of approximation. Strong BH cases (especially M31 and NGC 3115) are ones in which the derived M/L is higher than normal by an amount that is substantially larger than the uncertainties.

Progress in the BH search can come from improvements in analysis as well as in observations. In particular, we can exploit LOSVDs. Their calculation and use have been discussed elsewhere, e.g. by Bender (1990), Rix & White (1992), van der Marel & Franx (1993), Gerhard (1991, 1993a,b), Winsall & Freeman (1993), Kuijken & Merrifield (1993), Dehnen & Gerhard (1993, 1994), Saha & Williams (1994), Evans & de Zeeuw (1994), van der Marel et al (1994b), Bender et al (1994), and Statler (1995). It is convenient to measure departures from Gaussian LOSVDs using an expansion in Gauss-Hermite polynomials H_i (van der Marel & Franx 1993; Gerhard 1993a,b; Dehnen & Gerhard 1993):

$$\mathrm{LOSVD}(v) = \frac{\gamma}{\sqrt{2\pi\sigma^2}} e^{\frac{(v-V)^2}{2\sigma^2}} \left[1 + \sum_{i=3}^{n} h_i H_i \left(\frac{v - V}{\sigma} \right) \right], \qquad (2)$$

where γ is the line strength. If $h_3 < 0$, then the LOSVD has extra power on the systemic-velocity side of V. If h_4 is negative (positive), then the LOSVD is more square (triangular) than a Gaussian. The h_4 coefficient provides direct observational constraints on the velocity anisotropy: tangentially anisotropic models generally have $h_4 < 0$; radially anisotropic models generally have $h_4 > 0$ (e.g. Gerhard 1991, 1993a,b; van der Marel & Franx 1993; Dehnen & Gerhard 1993; van der Marel et al 1994b). Application of line-of-sight velocity distributions to the black hole search has been pioneered independently by R van der Marel and by O Gerhard and their collaborators. The following

sections discuss the added confidence provided by this second iteration in the analysis.

4.2 *M31* ($M_\bullet \simeq 3 \times 10^7\ M_\odot$)

M31 is the strongest BH case because of the rapid rotation and large velocity dispersion in its nucleus (Dressler 1984; Kormendy 1987a, 1988a,c; Dressler & Richstone 1988; Richstone et al 1990). Its dynamics have been measured by four independent groups. It is also the first galaxy for which we have made an iteration in improving the spatial resolution.

M31 contains the best known example of a nuclear star cluster (see Johnson 1961, Kinman 1965, Sandage 1971 for reviews) that is dynamically distinct from the bulge (Tremaine & Ostriker 1982). Light et al (1974) imaged it with *Stratoscope II*: At $\sigma_* \simeq 0''.1$, it is asymmetric; its axial ratio is $\simeq 0.6$, and the brightest spot is near the NE end. Lauer et al (1993) and Crane et al (1993b) observed it with *HST*; Lauer and collaborators show that the nucleus is double (Figure 4).

The rapid rotation of the nucleus (discovered by Lallemand et al 1960) and its steep central dispersion profile are shown in Figure 5. Dressler & Richstone (1988) and Kormendy (1988a,c) carried out analyses like those described in the previous section. These were complementary: Kormendy considered uncertainties in the light distribution (particularly its flattening) in more detail,

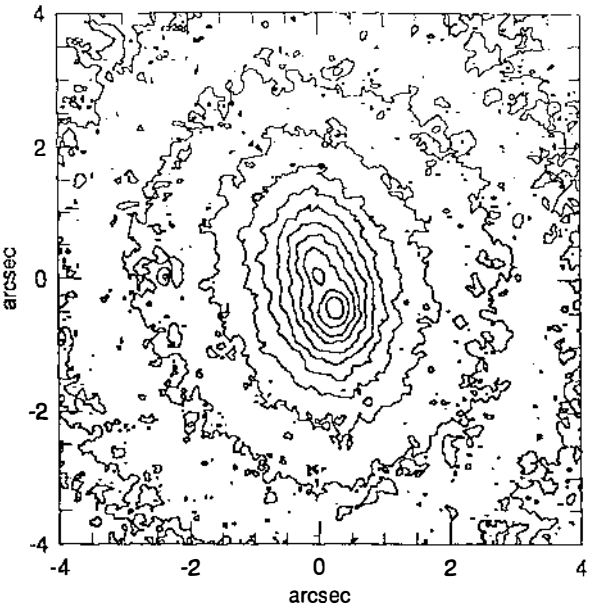

Figure 4 *HST* Planetary Camera *V*-band isophotes of the nucleus and inner bulge of M31 after Lucy deconvolution (Lauer et al 1993).

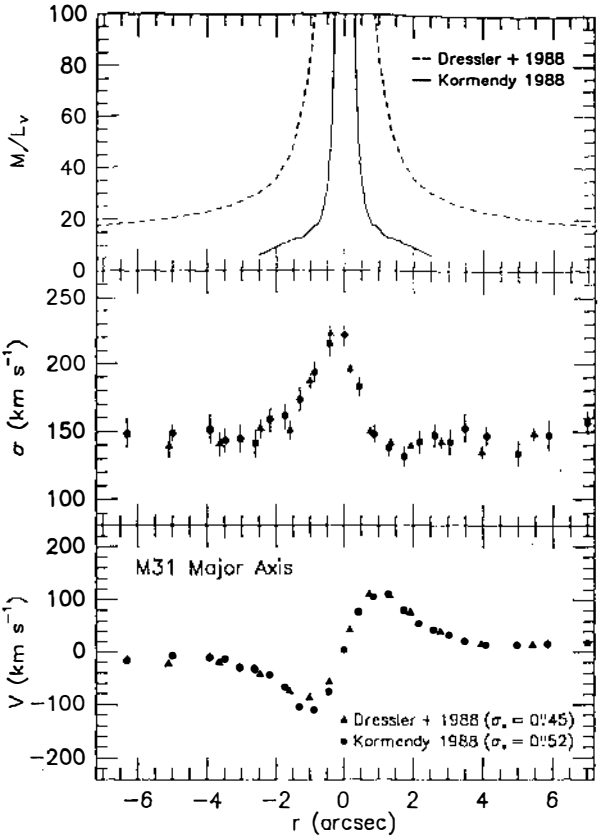

Figure 5 Rotation V, dispersion σ, and M/L ratio profiles in M31.

and Dressler & Richstone showed that the results are independent of velocity anisotropy. The mass-to-light ratio profiles are somewhat model dependent, but both papers showed that M/L_V rises near the center to values $\gtrsim 100$ (Figure 5). This implies that M31 contains an MDO of mass $M_\bullet \simeq 3 \times 10^7 M_\odot$.

The photometric asymmetry of the nucleus was known in 1988. Dressler, Richstone, and Kormendy also observed asymmetries in the velocity field but averaged over them in their analyses. The double nucleus complicates the BH case, so more detailed models should be constructed. However, it is unlikely that M/L_V is normal for an old stellar population: The observed velocities would have to overestimate the equilibrium virial velocities by a factor of $\sim$4. Instead, the *HST* observations are telling us something about the formation of the nucleus.

Lauer et al (1993) discuss possible explanations of the double nucleus; none is very attractive. Extinction is unlikely: There is no color gradient. M31 may have accreted and almost digested a compact elliptical like M32. However,

timescales are a problem. At $2r = 0''.49 = 1.7$ pc (the projected separation), a relative velocity of 200 km s^{-1} implies a circular orbit period of 50,000 y. Dynamical friction should result in a merger within a few orbital times. Are we just lucky to catch the nuclei *in flagrante delicto*? Two effects may reduce the dynamical friction. If P1 is accreted, it may fortuitously corotate with the stars of P2 (King et al 1995). Alternatively, both nuclei could be dominated by BHs. This scenario is ad hoc but not implausible. We do not know whether either effect is sufficient.

Finally, Tremaine (1995) has recently suggested a model in which the brightness enhancement at P1 is caused by an eccentric nuclear disk. This model requires that a $10^{7.3}$-$M_\odot$ BH dominate the potential, otherwise the lifetime of P1 against differential precession is short. The eccentric disk could result from an accretion but there are other possibilities too. An advantage of Tremaine's model is that it is specific enough to be testable with better kinematic measurements.

Bacon et al (1994) add new information about the asymmetries by presenting two-dimensional V and σ maps (Figure 6). They confirm the conclusion of Dressler & Richstone (1988) and of Kormendy (1988c) that the rotation curve of the nucleus is symmetric about its center ("P2" in Lauer et al 1993) and not about the brightest point ("P1"). All studies also agree that the center of the nucleus is the center of the bulge. However, this is not the point of maximum σ. Instead, the brightest and hottest points are displaced from the rotation center by similar amounts in opposite directions. Also, $\sigma(r)$ drops rapidly to or below the bulge dispersion on the brighter side of the nucleus. It is natural to wonder (Lauer et al 1993) whether P1 is cold. Then the displacement of the $\sigma(r)$ peak from P2 could be due to a contribution from P1 at the center.

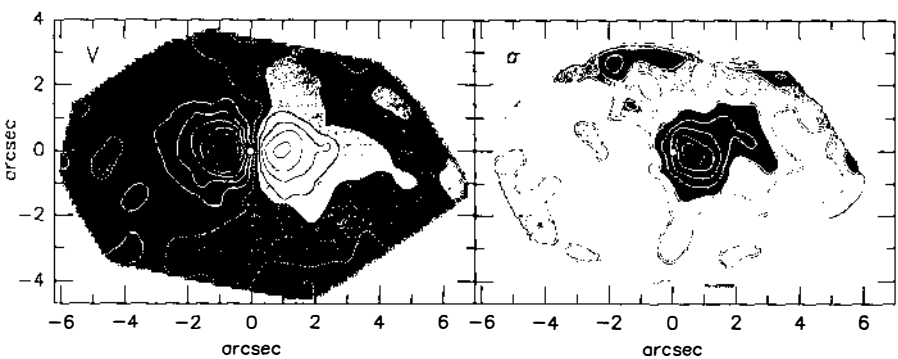

Figure 6 Contours of constant velocity (*left*) and velocity dispersion (*right*) in the nucleus of M31 (Bacon et al 1994). The range of velocities (*white* to *black*) is -120 km s^{-1} $\leq V \leq$ 120 km s^{-1} and 140 km s^{-1} $\leq \sigma \leq$ 240 km s^{-1}. These CFHT observations have spatial sampling $= 0''.39$ and resolution $\sigma_* \simeq 0''.37$. The major axis of the nucleus is horizontal; the white dot marks its photometric center.

LOSVD observations by van der Marel et al (1994a) are consistent with this interpretation. Using the William Herschel Telescope (WHT; slit width = 0.″45, $\sigma_* = 0.''32$), they show that the Gauss-Hermite coefficient $h_3(r)$ is opposite in sign to $V(r)$ with a strong negative peak, $h_3 \simeq -0.17$, near P1. This suggests that the LOSVD consists of a hot component that rotates slowly plus a cold one that rotates rapidly.

More definite conclusions require higher spatial resolution. This is expected from the new Subarcsecond Imaging Spectrograph (SIS) on the CFHT and from *HST*. No absorption-line spectroscopy is available yet from *HST*; however, a second iteration of spectroscopy on BH candidate galaxies is under way by Kormendy and collaborators using SIS.

SIS removes the main limitation of previous CFHT work: Herzberg Spectrograph resolution was limited by camera optics to FWHM $\geq 0.''7$. SIS optics are better than the seeing. The scale is $0.''0864$ pixel^{-1}; slit widths of $0.''3$ can be used. Tip-tilt guiding is incorporated; by offsetting the guide probe, the observer can center the object on the slit to one-pixel accuracy. As a result, the resolution is limited only by seeing and by telescope aberrations. A resolution of FWHM $\simeq 0.''45$ ($\sigma_* = 0.''19$) is reasonably common. Few objects are bright enough to be observed with *HST* at $< 0.''25$ resolution, so SIS remains useful in the *HST* era.

Figure 7 shows SIS measurements of the M31 nucleus (Kormendy & Bender 1995). The line-of-sight velocity distribution has two components. The steep central rise in σ seen by previous authors is a feature of P2: P2 is much hotter than the bulge near the center. But P1 is colder than the bulge at all radii. The LOSVDs and the V and σ fits imply that P1 has $\sigma \lesssim 85$ km s^{-1} at the center. This supports the idea that P1 is an accreted, low-luminosity stellar system. Since P1 overlaps P2 at the center, it also confirms that the $\sigma(r)$ asymmetry is due to the contribution of P1 at P2.

The accretion hypothesis can be tested. King et al (1995) have made a preliminary comparison of the stellar populations of P1 and P2 using a $\lambda \simeq 175$ nm image obtained with *HST*. In the UV, P2 has a higher surface brightness than P1. But the excess flux is small; it is equivalent to one post-asymptotic-branch giant star. King et al (1995) suggest that the excess flux is due to the central radio source (Table 1). They also confirm that P1 is compact (its brightness drops to zero at $r \simeq 0.''63$) and faint ($V \simeq 14.8$; $M_V \simeq -9.7$). P1 is no brighter than a large globular cluster, although it is much denser. Most interestingly, King et al (1995) see no sign that the (UV − optical) color of P1 is different from that of the bulge. This does not favor accretion. On the other hand, P1 nowhere contributes more than 55% of the total surface brightness. It is difficult to measure its metallicity free of contamination from P2. It will be important to see whether *HST* shows a drop in spectral line strengths at P1.

HST will also be important for the black hole case. Meanwhile, the dramatic kinematics seen with SIS (Figure 7) support the BH detection.

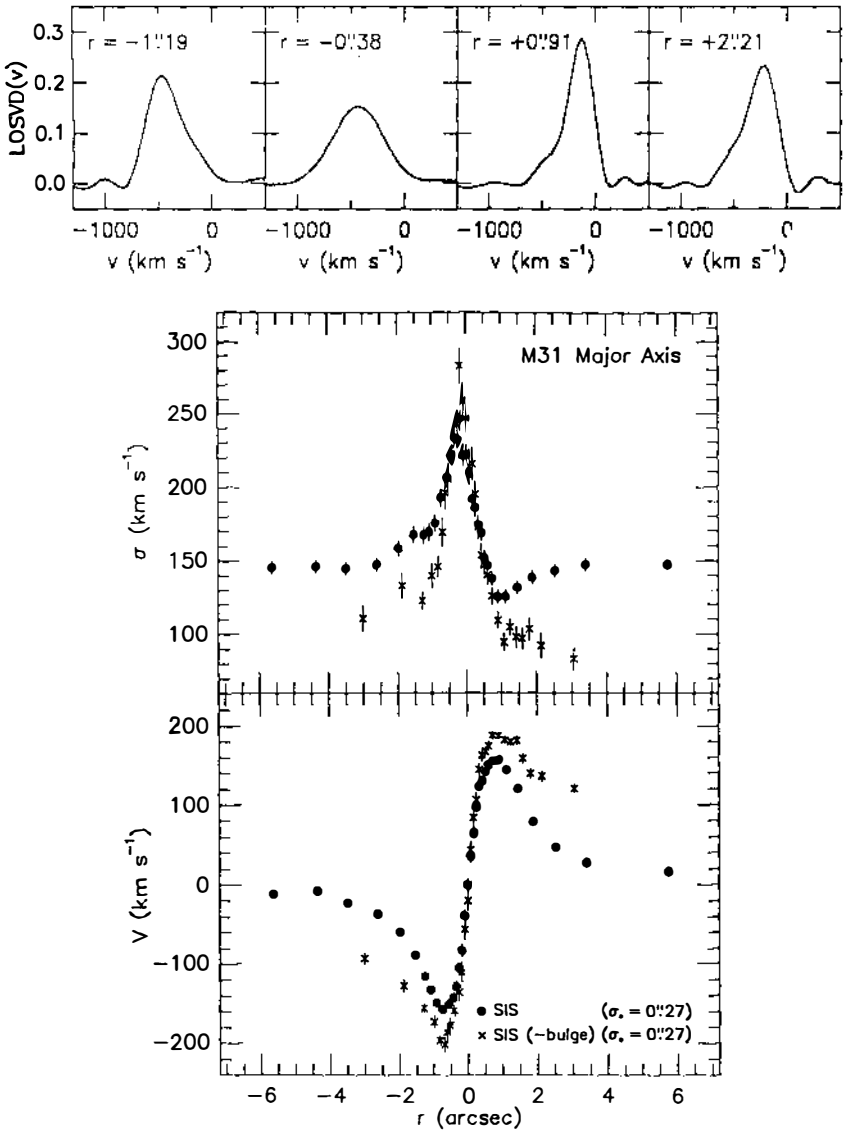

Figure 7 Line-of-sight velocity distributions (*top*) and $V(r)$ and $\sigma(r)$ profiles (*bottom*) along the nucleus major axis of M31 (Kormendy & Bender 1995). Filled circles show the kinematics of the nucleus plus bulge as observed; crosses show the nuclear kinematics after the bulge spectrum is subtracted.

4.3 *NGC 3115 ($M_\bullet \simeq 1 \times 10^9\ M_\odot$)*

NGC 3115 is a edge-on S0 galaxy (Sandage 1961) whose bulge contributes 94% of the total light (Capaccioli et al 1987). At $M_B = -19.9$, the bulge is almost as bright as a giant elliptical, but it rotates rapidly enough to be nearly isotropic (Illingworth & Schechter 1982). Kormendy & Richstone (1992, hereafter KR92) showed that its steep central kinematic gradients (Figure 8) make NGC 3115 the strongest BH case after M31.

KR92 derived dynamical models that bracket the observations after projection and seeing convolution. Figure 8 (*left*) illustrates the best-fitting isotropic model at three spatial resolutions. The $\sigma_* = 0\farcs44$ lines are for the resolution of the KR92 observations; by construction, they fit the open circles. One iteration of improved spatial resolution is now available. The filled circles in Figure 8 show CFHT SIS measurements obtained with a $0\farcs3$ slit. At $\sigma_* = 0\farcs244 \pm 0\farcs015$, $V(r)$ already reaches its asymptotic value at $1''$, and the apparent central velocity dispersion has risen from 295 ± 9 km s^{-1} to 343 ± 19 km s^{-1}. This is almost exactly the increase predicted by the KR92 models. The middle lines show the best-fitting isotropic model at $\sigma_* = 0\farcs244$. It fits the rotation

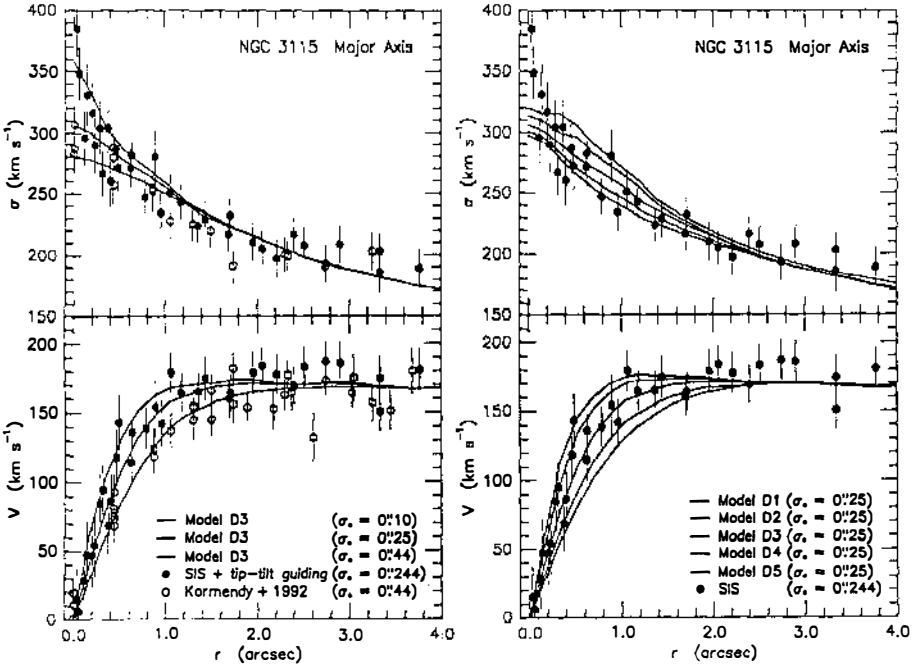

Figure 8 (*Left*) Kinematics of NGC 3115 compared with the best-fitting isotropic model (D3) from KR92 as seen at various spatial resolutions. (*Right*) SIS data compared with isotropic models D1–D5 from KR92 as seen at $\sigma_* = 0\farcs25$.

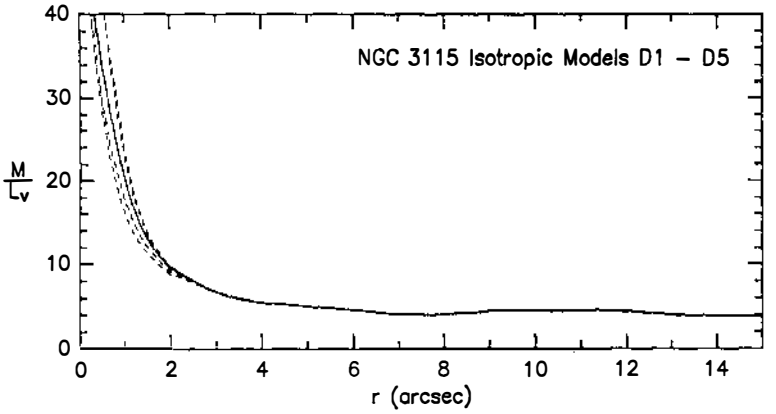

Figure 9 Mass-to-light ratio interior to radius r for the isotropic models in Figure 8. All models have $M/L_V \simeq 4$ at $r \simeq 4''$ to $24''$; this value is normal for a bulge of $M_B = -19.9$ (Kormendy 1987b, Figure 3). In contrast, M/L_V increases at $r < 2''$ by a factor of $\gtrsim 10$. (From KR92.)

curve well, and it falls slightly below the dispersion profile at the center. Also, the isotropic models continue to bracket the data at the improved resolution (Figure 8, *right*). These models imply that M/L_V rises toward the center to values much larger than those of old stellar populations (Figure 9). Note that M/L_V has already risen by a factor of 5 at $1''$; contrary to the claim of Rix (1993), this is not a marginal MDO detection. In fact, the MDO dominates gravitationally to $r_\bullet = GM_\bullet/\sigma^2 \gtrsim 1''.8$. We see that $r_\bullet \gg \sigma_*$. If the M/L_V gradient is due to a central dark mass added to stars with constant $M/L_V(r)$, then $M_\bullet \simeq 10^9\ M_\odot$. The dark mass can be reduced by allowing σ_r to be larger than σ_θ or σ_ϕ near the center (Equation 1), but KR92 showed that $M_\bullet$ must be $\gtrsim 10^8\ M_\odot$ or the models predict too little rotation at $r \simeq 1''$ to $2''$. We conclude that a significant iteration in spatial resolution confirms the BH case. This increases our confidence in the MDO detection.

Finally, the top curves in each panel of Figure 8 (*left*) show the best-fitting isotropic model from KR92 at *HST* resolution ($0''.25$ aperture used with the Faint Object Spectrograph). Kormendy et al (1995a) observed NGC 3115 with *HST* in December 1994. They will combine the results with the SIS data and will construct new dynamical models. It is reasonable to expect that these observations will complete step 1 of the BH search for NGC 3115, i.e. they should tell us definitively whether or not an MDO is present.

What caveats remain?

DUST ABSORPTION *HST* shows no dust near the center (Lauer et al 1995). The central color gradient is normal, and the galaxy is only weakly detected by the *IRAS* satellite (see KR92). The brightness profile is also normal (KR92, Lauer

et al 1995, Faber et al 1995). For dust to produce high M/L ratios, the central profile and parameters would have to be unlike those in any other galaxy and then made to look normal only because of absorption. This is implausible.

NUCLEAR BARS Gerhard (1988, 1989) has suggested that nuclear disks are really bars. When these are oriented end-on, we see stars near the pericenters of elongated orbits, so we measure rotation velocities that are larger than circular. This reduces the mass implied by the rotation curve. We do not know whether constant-M/L nuclear bar models can be constructed. However, we know enough about bars to conclude that they are implausible: (*a*) Noncircular streaming velocities have been measured in the SB0 galaxy NGC 936 (Kormendy 1983). This has an unusually strong bar, but departures from circular motions are only ±20%. Even if this bar were viewed end-on and even if all of the light came from the bar, the error in $M(r)$ from the V^2r/G term in Equation 1 would be only 40%. The σ^2r/G term would be unaffected: Kormendy saw no dispersion anisotropy in NGC 936. (*b*) In NGC 3115, the end-on nuclear bar would have a true major-axis radius of $\gtrsim 4''$, because $1''$ (where M/L_V looks large) is a pericenter radius. Such a bar would easily be seen in more face-on galaxies. Although some galaxies have nuclear bars (see Kormendy 1982 for a review), we have never seen one as elongated as the main bar in NGC 936, and argument (*a*) suggests that even this is not enough. Nevertheless, nuclear bar models should be investigated (Gerhard 1992).

VELOCITY ANISOTROPY Velocity anisotropy should be explored in more detail. That is, the limitations in maximum entropy models noted in Section 4.1 should be removed. For NGC 3115, this will be done in Kormendy et al (1995a).

LINE-OF-SIGHT VELOCITY DISTRIBUTIONS LOSVDs provide new constraints on the mass distribution that we are only beginning to use in the BH search (Gerhard 1993b; van der Marel et al 1994a,b; van der Marel 1994a,b; Dehnen 1995; Qian et al 1995). van der Marel et al (1994a) and Bender et al (1994) show that the LOSVDs in rotating systems are usually asymmetric, with extra wings on the systemic-velocity side of the mean V. That is, $h_3(r)$ and $V(r)$ have opposite signs. For NGC 3115, $h_3 \simeq -0.05$ at $r \lesssim 5''$. The above authors emphasize that $V(r)$ as derived by fitting a Gaussian to the LOSVD then overestimates the true velocity moment in Equation 1. van der Marel et al (1994a) worry that this accounts for the failure of constant-M/L models to fit the kinematics. Similarly, the true velocity dispersion is underestimated when the LOSVD has large wings (van der Marel 1994a,b). Bender et al (1994; see their figure 3) provide the necessary corrections ΔV and $\Delta\sigma$. At $0''.5 \lesssim r \lesssim 5''$ in NGC 3115, $\Delta V \simeq -14$ to -21 km s^{-1}. The important point is that ΔV is almost independent of radius. *The corrected rotation curve then reaches a slightly lower asymptotic value at* $r \simeq 1''$ *to* $5''$. *However, model rotation curves are always scaled to the asymptotic* V; *this is how the global* M/L

ratio is derived. Thus the main result of the correction is to lower the global (*i.e. bulge*) M/L_V. The change is only ~8%. It is small partly because less than half of $M(r)$ as derived from Equation 1 is due to $V(r)$; the dispersion profile is almost unchanged by the LOSVD correction. *The strength of the BH case is essentially unaffected, because the shape of the rotation curve is almost unchanged.* These remarks are reassuring. Nevertheless, as van der Marel et al (1994a) emphasize, KR92 did not check whether the LOSVDs of their models fit those of the galaxy. Models of NGC 3115 that exploit LOSVDs are planned (Kormendy et al 1995a).

M/L RATIOS The most serious caveat remains the fact that large M/L ratios do not uniquely imply a BH. Only step 1 of the BH search—the detection of an MDO—is nearing completion. We cannot exclude the possibility that galaxies contain central clusters of stellar remnants or brown dwarf stars. However, old stellar populations have remarkably consistent mass-to-light ratios, $M/L_V \simeq 1$ to 10, with $M/L_V \propto L^{0.2}$ (Kormendy 1987a,b; Faber et al 1987; Djorgovski et al 1988; Bender et al 1992, 1993). The increase of M/L_V with L is due to three effects: the metallicity-luminosity correlation (Faber 1973; more luminous galaxies are more metal-rich, so stars emit less V-band light per unit mass because of stronger absorption-line blanketing), the anisotropy-luminosity correlation (Davies et al 1983), and an age-luminosity correlation (Faber et al 1992). Given that old stellar populations contain stars with very large and very small mass-to-light ratios, it is surprising that the scatter in M/L is so small. But the small scatter is the reason why we interpret large nuclear M/L ratios as implying MDOs. Stellar densities in NGC 3115 are not outside the range observed in galaxies that lack MDOs or in globular clusters. These have normal populations. The spectra and colors of NGC 3115 also are normal. Therefore, we have no reason to expect a dramatic population gradient, and we see no evidence of one. An extreme population gradient would be required: Inside 1″, the dark star cluster would need to have about five times as much mass as the visible stars. Therefore, the most plausible conclusion is that NGC 3115 contains a central BH of mass $M_\bullet \sim 10^9\ M_\odot$.

To summarize: In NGC 3115, as in M31, the detection of an MDO is probably secure. But the arguments that we are detecting a black hole are not rigorous.

4.4 *M32* ($M_\bullet \simeq 2 \times 10^6\ M_\odot$)

The first galaxy with convincing evidence for an MDO was the dwarf elliptical M32; it is now the most thoroughly studied BH candidate. Like M31, it was long ago known to rotate rapidly near the center (Walker 1962). Dressler (1984) and Tonry (1984, 1987) measured its rotation curve with $\sigma_* \simeq 0\farcs5$ to $0\farcs85$ seeing at the Hale telescope; they demonstrated that the velocity dispersion rises significantly toward the center. Tonry (1984, 1987) fitted his data with isotropic dynamical models; these imply that M/L increases toward

the center. He concluded that M32 contains a BH of mass $M_\bullet \simeq$ (3 to 10) $\times 10^6\ M_\odot$.

These results were strengthened by Dressler & Richstone (1988), who obtained $\sigma_* \simeq 0\farcs5$ observations of M32 with the Hale telescope. Using the techniques of Section 4.1, they showed that velocity anisotropy provides no escape from the conclusion that an MDO is present. More detailed analysis by Richstone et al (1990) further supported the case.

Figure 10 illustrates the kinematics.

The conclusions of Tonry, Dressler, and Richstone have now been confirmed by three independent groups. These groups provide a significant iteration in spatial resolution over the discovery observations, and they strengthen the analysis by fitting LOSVDs. Therefore, M32, along with M31 and NGC 3115, is among the most secure BH candidates.

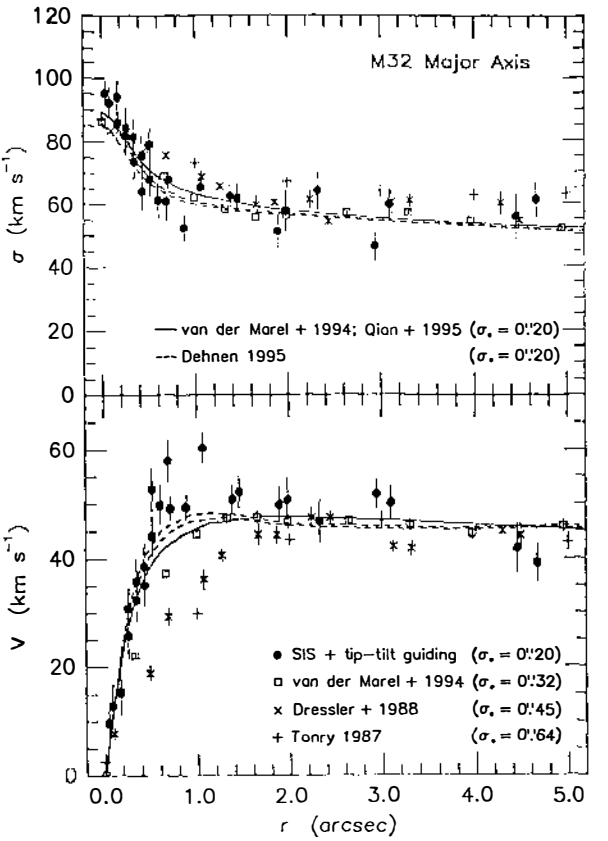

Figure 10 Kinematics of M32 compared with the dynamical models of van der Marel et al (1994b), of Qian et al (1995), and of Dehnen (1995) kindly recalculated by the above authors for $\sigma_* = 0\farcs20$.

Carter & Jenkins (1993) observed M32 with the WHT, a 0.″45 slit, and $\sigma_* = 0.''34$. At this resolution, $V(r)$ flattens out to 50 km s^{-1} at $\sim 1''$. Carter & Jenkins do not use the dispersion profile to measure masses, but they note that a high central M/L does not follow from $V(r)$ alone.

van der Marel et al (1994a) present additional WHT observations, including measurements of Gauss-Hermite coefficients. As in other rotating galaxies, h_3 and V have opposite signs; $h_3 \simeq -0.07$ at $r \gtrsim 1''$. Coefficients h_4–h_6 are nearly zero. van der Marel and collaborators note that Tonry's (1987) isotropic models do not fit $h_3(r)$; in fact, they have $h_3 \simeq 0$ at all radii. This demonstrates an interesting result: The LOSVDs are intrinsically asymmetric; they are not Gaussians rendered asymmetric by rotational line broadening, projection, or seeing. This is important for modelers who try to decipher the galaxy's dynamics. However, it does not have a large effect on the BH search, contrary to worries expressed in van der Marel's paper. This can again be seen by correcting the Gaussian-fit rotation velocities to velocity moments appropriate for Equation 1 using Figure 3 in Bender et al (1994). Because $h_3 \simeq$ constant at $r \gtrsim 1''$, $\Delta V \simeq -7$ km s^{-1} is nearly independent of radius [see also figure 2 in Rix (1993)]. Thus, the main effect of the correction is again to lower the bulge M/L. This is confirmed by detailed analysis, as decribed below.

van der Marel et al (1994b) construct M32 models with two-integral distribution functions $f(E, L_z)$, where E is total energy and L_z is the axial component of angular momentum. Without MDOs, these models fit $V(r)$ and $h_3(r)$–$h_6(r)$, but they fail to fit the central dispersion gradient. In fact, they predict that σ falls toward the center at $r < 1''$. [Physically: If stars cannot climb out of their own potential well and therefore make a cuspy profile, they must be cold; see, e.g. Binney (1980), Dehnen (1993), Tremaine et al (1994).] Similar results are obtained with a moment equation analysis that fits V, σ, and the skewness of the LOSVDs. Good fits to $\sigma(r)$ are obtained when an MDO of mass $M_\bullet = (1.8 \pm 0.3) \times 10^6\ M_\odot$ is added. These results are in good agreement with the conclusions of Tonry, Dressler, and Richstone.

Qian et al (1995) take the moment equation models one step further by calculating their distribution functions using the contour integral method of Hunter & Qian (1993). They can then derive the complete LOSVDs and not just their skewness. For the $M_\bullet = 1.8 \times 10^6\ M_\odot$ model, the comparison to V, σ, and h_3–h_6 shows remarkably good agreement along all slit positions measured by van der Marel et al (1994b).

Dehnen (1995) has made further $f(E, L_z)$ models of the van der Marel et al (1994a) observations using a slightly different technique. He recovers $f(E, 0)$ from ρ using a Richardson (1972)–Lucy (1974) algorithm. The distribution function is then multiplied by a guessed function of L_z and used to calculate V, σ, and h_3–h_6. These are compared to the observations, and the distribution function is iterated until it agrees with all observables. Slit width, pixel size,

and seeing are taken into account. Dehnen's results are closely similar to those of van der Marel et al (1994b). In particular, he confirms that such models do not fit the kinematics unless they contain an MDO of mass $M_\bullet \simeq (1.6 \text{ to } 2) \times 10^6$ $M_\odot$. Again, the models with an MDO provide an excellent fit to $h_3(r)$–$h_6(r)$ along the major, minor, skew, and offset axes.

van der Marel et al (1994b), Qian et al (1995), and Dehnen (1995) improve on earlier analyses in several important ways. The models are properly flattened, they fit the non-Gaussian LOSVDs, and they fit kinematic observations at a variety of slit positions, not just along the major axis. The latter point is important: As van der Marel et al (1994b) point out, Tonry's (1984, 1987) models explain the major-axis dispersion gradient as due to rotational line broadening, but without an intrinsic dispersion gradient, they cannot be in dynamical equilibrium along the minor axis. The $f(E, L_z)$ models solve this problem.

These models also have an important shortcoming compared to the models of Dressler & Richstone (1988). The distribution functions are restricted to be functions of two integrals; in many cases, they are required to be analytic. We can show that these models fail to fit the data without a BH, but we cannot prove that it is impossible to find a more general distribution function that succeeds without a BH. In contrast, the maximum entropy models can be forced to have the smallest possible M/L as $r \to 0$. When this fails—subject to shortcomings discussed in Section 4.1—an MDO is required. Thus, the distribution function and maximum entropy models are complementary: Each has strengths that the other lacks. It is reassuring that they agree. But an exploration of extreme models that successfully fit V, σ, and h_n without the limitations of published maximum entropy models is still needed.

Finally, Figure 10 shows new observations of M32 obtained with the CFHT and SIS (Kormendy et al 1995a). These provide a further improvement in spatial resolution: The slit width was 0.″35, and the seeing σ_* was 0.″20. At this resolution, the central rotation curve is much steeper; it peaks at $V \simeq 53 \pm 2$ km s^{-1} at $r \simeq 0.''85$. The central dispersion profile is slightly steeper; $\sigma(0) \simeq 94 \pm 2$ km s^{-1}. Figure 10 compares the SIS data with the models of van der Marel et al (1994b), Qian et al (1995), and Dehnen (1995) as seen at the present resolution. The fit is good at large radii. But $V(r)$ and $\sigma(r)$ both reach higher maximum values than the models predict. Therefore, the black hole case gets stronger at SIS resolution. Modeling of the SIS data is in progress.

In summary, five independent groups have observed and modeled M32. Models without MDOs consistently fail to fit the kinematics. These include maximum entropy models that were instructed to minimize the central M/L. Successful models require that $M_\bullet \simeq 2 \times 10^6$ $M_\odot$. This result has survived improvements in spatial resolution of a factor of three since the MDO discovery. Given expectations based on Figure 10 and on the predictions of Dehnen

(1995) and Qian et al (1995), *HST* spectroscopy is feasible. van der Marel et al (1995) plan to make these observations. Meanwhile, the case for an MDO is already strong.

4.5 *NGC 4594—The Sombrero Galaxy ($M_\bullet \simeq 5 \times 10^8\ M_\odot$)*

The remaining stellar-dynamical BH cases (Sections 4.5–4.7) are weaker than those of M31, M32, and NGC 3115 because the modeling analyses have explored fewer degrees of freedom on $M(r)$.

NGC 4594 is an almost edge-on Sa galaxy illustrated in the *Hubble Atlas* (Sandage 1961). Its bulge is as luminous as a giant elliptical ($M_B \simeq -21.2$ at 9.2 Mpc distance), but it rotates rapidly enough so that velocity anisotropies are small (Kormendy & Illingworth 1982). This reduces the uncertainties in the mass measurements.

Kormendy (1988d) observed NGC 4594 with the CFHT (slit width = 0.″5, scale = 0.″435 pixel^{-1}, seeing $\sigma_* = 0.''40$). The central kinematics reveal a nuclear disk: At $r \simeq 5''$, the rotation curve has an inner peak, and the dispersion profile has a minimum ($\sigma = 181 \pm 6$ km s^{-1}) that is significantly lower than the bulge dispersion ($\sigma \simeq 240$ km s^{-1}). The nuclear disk is also detected photometrically (Burkhead 1986, 1991, Kormendy 1988d, Crane et al 1993b, Emsellem et al 1994a). Its presence guarantees that the line-of-sight velocity distributions are asymmetrical. But the disk is well localized and significantly brighter than the bulge. At $r \simeq 10''$ to $15''$, both the photometry and the kinematics suggest that the disk is negligible; here, the major-axis dispersion is equal to that along the minor axis. Therefore, Kormendy subtracted the bulge spectrum obtained from the minor axis and scaled to the major-axis bulge profile. He then confined his analysis to the kinematics of the nuclear disk. This is a well-defined kinematic subpopulation that can be used in Equation 1 to measure the total mass distribution. Recently, Kormendy (1994) has shown that asymmetries in the LOSVDs due to superposition of the nuclear disk and bulge were removed by the decomposition; the Kormendy (1988d) models are an adequate fit to the residual LOSVDs.

The machinery of Section 4.1 was used to derive unprojected rotation velocity, velocity dispersion, and brightness profiles that bracket the bulge-subtracted data after projection and seeing convolution. The solutions imply that the mass-to-light ratio rises from normal values, $M/L_V \simeq 7.8$, at large radii to $M/L_V > 100$ near the center. (All values in this section have been corrected to the distance scale of Table 1.) Kormendy & Westpfahl (1989) showed that the outer M/L_V remains constant to $\sim 180''$. Therefore, a normal, old stellar population dominates the bulge over a large radius range. However, an MDO is present at $r < 1''$; if $M/L_V(r) =$ constant for the stellar population, then $M_\bullet \simeq 5 \times 10^8\ M_\odot$.

The main shortcoming of the analysis was that velocity anisotropy was not explored. The rapid rotation and the nuclear disk make it unlikely that

$\sigma_r \gg \sigma_{\text{tangential}}$ (Kormendy & Illingworth 1982; Jarvis & Freeman 1985). Nevertheless, anisotropic models should be constructed.

The kinematics of NGC 4594 have been confirmed by five independent groups. Jarvis & Dubath (1988) observed the galaxy with the ESO 3.6-m telescope, a 2″ slit, 1.″17 pixels, and seeing $\sigma_* \simeq 0.''51$ to $0.''64$. Their data agree well with Kormendy's. They estimate the total mass within 3.″5 of the center to be $7 \times 10^8\ M_\odot$ and "conclude that there is strong evidence that NGC 4594 contains a super-massive object, possibly a black hole or massive star cluster." However, they did not calculate M/L ratios, so they cannot tell how much of the mass is dark. In fact, comparably luminous galaxies typically have core masses $>10^9\ M_\odot$ *in stars* (e.g. Kormendy 1982, table 3). In NGC 4594, the luminosity inside 3.″5 is $L_V \simeq 6 \times 10^8\ L_\odot$ (Kormendy 1988d, figure 10), and $M/L_{V,\text{bulge}} \simeq 7.8$. So Jarvis & Dubath underestimate the mass inside 3.″5.

Using the ESO 2.2-m telescope, with 1.″87 pixels and a 2″ slit, Wagner et al (1989) were the first to examine LOSVDs. These clearly show a superposition of rapidly rotating, cold and slowly rotating, hot components. The cross-correlation peaks at the center and at $\pm 3.''6$ agree well with those illustrated in Kormendy (1994). Wagner et al (1989) derive a seeing-corrected mass of $(3 \pm 1.2) \times 10^9\ M_\odot$ inside 3.″8 radius, but like Jarvis & Dubath (1988), they do not derive M/L ratios.

The kinematics were further confirmed by Carter & Jenkins (1993), using the WHT, with 0.″34 pixels, a 0.″55 slit, and seeing $\sigma_* \simeq 0.''51$. They remark that rotation alone is not rapid enough to imply a large mass-to-light ratio. It is true that the central rise in M/L found by Kormendy (1988d) is largely due to the dispersion gradient. Checking anisotropy is probably more important than Kormendy suggested.

van der Marel et al (1994a) took additional spectra with a 1.″25 slit, 0.″6 pixels, and seeing $\sigma_* = 0.''47$. These spectra agree with previous results. The main new contribution is the measurement of LOSVDs. The maximum amplitude of $h_3 = -0.15$ is reached at $r = 6''$; $|h_3|$–$|h_6|$ then fall almost to zero at $r = 10''$–$20''$. This is in excellent agreement with the Kormendy (1988d) and Burkhead (1991) conclusion that the nuclear disk dominates near the center but is negligible at intermediate radii.

In summary, the kinematics of NGC 4594 are well confirmed. But none of the published measurements improves on the discovery resolution.

Also, there has been little progress in modeling. Emsellem et al (1994a) model the Kormendy data using multi-Gaussian expansions of the point-spread function and galaxy light distribution. Again, isotropic models do not fit the dispersion profile unless there is an MDO of mass $5 \times 10^8\ M_\odot$. However, even the MDO model rotates too slowly. Part of the problem is that Emsellem and collaborators fit the composite (not bulge-subtracted) kinematics; this adds to the uncertainties because of the messy LOSVDs.

More definitive results on NGC 4594 should be available soon. Emsellem et al (1994b) have obtained two-dimensional spectroscopy with 0.″39 spatial sampling on the CFHT. Kormendy et al (1995a) have taken CFHT SIS spectra with $\sigma_* = 0.''27$; at this resolution, the apparent central velocity dispersion is 282 ± 8 km s^{-1}. They also observed NGC 4594 with *HST* in February 1995. The issue of whether NGC 4594 contains an MDO should be settled soon.

4.6 *The Milky Way Galaxy ($M_\bullet \simeq 2 \times 10^6\ M_\odot$)*

The center of our Galaxy is enormously complicated and well studied. Excellent reviews (Genzel & Townes 1987, Morris 1993, Genzel et al 1994a) and conferences proceedings (Backer 1987, Morris 1989, Genzel & Harris 1994) discuss the physics in detail. Papers on a possible Galactic BH include those by Lynden-Bell & Rees (1971), Rees (1987), Phinney (1989), and de Zeeuw (1993). Here we summarize the AGN evidence and gas dynamics briefly and then concentrate on the stellar-dynamical BH search.

The radio source Sgr A* (Genzel et al 1994a, figure 2.2) is assumed to be the Galactic center; this is not certain. Sgr A* is spectacularly tiny. Lo et al (1985) measure a radius of $\theta < (1.1 \pm 0.1) \times 10^{-3}$ arcsec = 9 AU at $\lambda = 1.3$ cm wavelength. Also, $\theta \propto \lambda^2$ because of interstellar electron scattering. Strong limits require short λ; at 3 mm, $\theta \lesssim 0.07 \times 10^{-3}$ arcsec = 0.6 AU (Rogers et al 1994). This is only 15 times the Schwarzschild radius of the $2 \times 10^6\ M_\odot$ MDO suggested by the dynamics. It is easy to be impressed by the small size. But as an AGN, Sgr A* is feeble: Its radio luminosity is 10^{34} erg s^{-1} $\sim 10^{0.4}\ L_\odot$. The infrared and high-energy luminosity is much higher (Genzel et al 1994a), but there is no compelling need for a 10^6-$M_\odot$ BH. Mini-AGNs caused by stellar-mass engines are known (e.g. Mirabel et al 1992). So, to find out whether the Galaxy contains a supermassive black hole, we need dynamical evidence.

Genzel & Townes (1987) and Genzel et al (1994a) review the dynamics of neutral and ionized gas near the Galactic center. Velocities of 100–140 km s^{-1} imply masses of several $\times 10^6\ M_\odot$ inside 1 pc (Figure 11) *if the gas is in circular motion*. This assumption is not well motivated: As discussed in Genzel et al (1994a), stellar winds from luminous young stars combine to make a wind blowing out of the central parsec; a few hundred supernovae are thought to have occurred in the central 10^2 pc in the past 10^4–10^5 y; and some noncircular motions are seen, including an expanding bubble of hot gas (Eckart et al 1992). It is surprising that the motions are so close to gravitational. Without confirmation from stellar dynamics, we would not dare to include the Galaxy in Table 1.

Because of optical extinction, stellar velocities are usually measured using K-band CO band heads. From the first papers (Sellgren et al 1987, Rieke & Rieke 1988), masses of 10^6–$10^7\ M_\odot$ at $r \lesssim 1$ pc were deduced. McGinn et al (1989) and Sellgren et al (1990) measured spectra of integrated starlight in apertures of 2.″7–20″ diameter. The rotation curve rises in the inner 15″ = 0.6

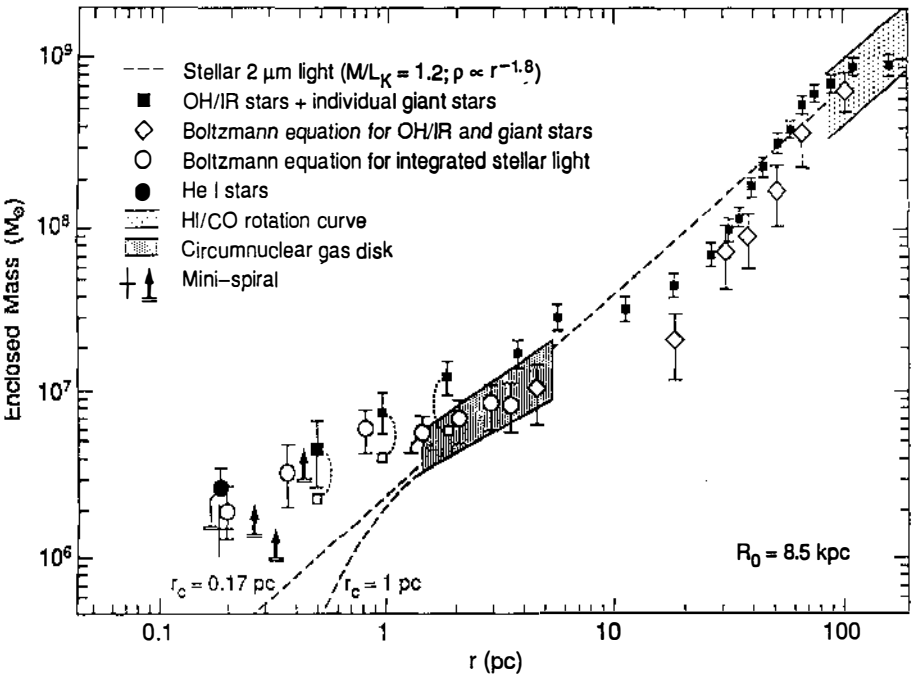

Figure 11 Galactic center mass distribution (Genzel et al 1994a). The points show dynamical masses derived from various kinematic tracer populations (see text). For two possible core radii, the dashed lines show the mass distribution in stars derived from the K-band brightness distribution assuming $M/L_K = 1.2$.

pc and then flattens out at $V \simeq 36$ km s^{-1}. The projected dispersion rises from ~70 km s^{-1} at $r > 35''$ to 125 km s^{-1} at $r < 20''$. Interestingly, the CO band strength decreases at small radii; the true strength is consistent with zero at $r < 15''$. The authors suggest that the atmospheres of giant stars have been modified (stripped off?) in the dense environment of the nucleus. This limits the resolution to 0.6 pc, which is not much better than ground-based resolutions in M31 and M32. Neglecting projection and anisotropy and assuming that the core radius $r_c = 0.4$ pc, McGinn et al (1989) conclude that the mass distribution is inconsistent with the light distribution; it requires $M_\bullet \simeq 2.5 \times 10^6\ M_\odot$. Sellgren et al (1990) derive $M_\bullet \simeq (5.5 \pm 1.5) \times 10^6\ M_\odot$.

The best dynamical analyses are by Kent (1992) and by Evans & de Zeeuw (1994). Kent notes that the central K-band starlight is a flattened power law, $\nu \propto r^{-1.85}$. He constructs a flattened, isotropic Jeans equation model that fits the stellar and gas kinematics along the major and minor axes. This requires an MDO of mass $M_\bullet \simeq 3 \times 10^6\ M_\odot$. Evans & de Zeeuw (1994) make $f(E, L_z)$ models for the same power-law density distribution; these fit the kinematics if $M_\bullet \simeq 2 \times 10^6\ M_\odot$.

Kinematic measurements of a number of kinds of stars confirm these results [e.g. OH/IR stars: Lindqvist et al (1992); He I stars: Krabbe & Genzel (1993), quoted in Genzel et al (1994)]. The dynamical mass distribution is compared to that derived from the infrared light distribution in Figure 11. Gas and stellar kinematics agree remarkably well. The conclusion that there is (1 to 3) $\times 10^6$ $M_\odot$ of central dark matter even looks robust with respect to the poorly known core radius of the stars.

Haller et al (1995) have remeasured the kinematics with a 1.″3 slit placed at several positions near Sgr A*. From He I lines in hot stars and CO band heads in cool stars, they find masses at $r < 1$ pc that are somewhat lower than those reviewed by Genzel et al (1994a). Haller and collaborators raise the possibility that some of the dark matter near the center may be extended in radius. Then $M_\bullet \simeq$ (1 to 2) $\times 10^6$ $M_\odot$.

Most recently, Krabbe et al (1995) have obtained two-dimensional K-band spectroscopy of the central $8'' \times 8''$ at FWHM = $1''$ resolution. From 35 individual stellar velocities (mostly based on emission lines), they derive $\sigma = 153 \pm 18$ km s^{-1} at $\langle r \rangle = 0.245$ pc and hence $M_\bullet \simeq 3 \times 10^6$ $M_\odot$. If the velocity distribution is approximately isotropic, the case for a high central mass-to-light ratio is quite strong.

Nevertheless, the Galactic center BH case is fundamentally more uncertain than those of the best candidates. The observations are sensitive to discreteness and population effects. Absorption-line measurements are not luminosity-weighted along the line of sight because the CO bands disappear in the central 0.5 pc. It is hard to be confident that a particular kinematic tracer is distributed in radius like the 2.2 μm light (which is used to determine $d \ln \nu / d \ln r$ and the stellar mass distribution). Given the peculiar (young?, rejuvenated?) stellar population, it is not clear that M/L_K is constant for the stars. Also, no models have explored anisotropy. On the other hand, we can hope for better spatial resolution than in any other galaxy. The case for an massive dark object is strong enough to be taken seriously. But further work is needed.

If the Galaxy contains a black hole, it is starving in a blizzard of food. This could be embarrassing (Section 7).

4.7 *NGC 3377 ($M_\bullet \simeq 8 \times 10^7$ $M_\odot$)*

NGC 3377 is a normal elliptical galaxy illustrated in the *Hubble Atlas*. At $M_B = -18.8$, it rotates rapidly enough to be nearly isotropic. Its core is tiny, so small radii have large luminosity weight in projection. The axial ratio is 0.5; because no elliptical is much flatter, NGC 3377 must be nearly edge-on. Finally, the distance is only 9.9 Mpc. Therefore, NGC 3377 is an excellent target for a BH search.

Kormendy et al (1995b; see also Kormendy 1992a) observed NGC 3377 with the CFHT and resolution $\sigma_* \simeq 0.''48$. The galaxy is kinematically similar to M32: $V(r)$ rises rapidly near the center to 100 km s^{-1} and then levels off;

$\sigma(r) \simeq 90$ km s^{-1} at $r \gtrsim 2''$ and then rises to 158 ± 11 km s^{-1} at the center. The kinematics are confirmed by Bender et al (1994). Kormendy et al (1995b) show that isotropic kinematic models require an MDO of mass $M_\bullet \simeq 8 \times 10^7 M_\odot$. They also fail to find anisotropic models that fit without an MDO, but the failure is not large. Therefore, this is a weak MDO detection. After M32, NGC 3377 is only the second elliptical galaxy with stellar-dynamical evidence for an MDO.

4.8 *M33 ($M_\bullet \lesssim 5 \times 10^4 M_\odot$)*

One black hole upper limit deserves discussion. M33 is a bulgeless Sc galaxy with a nucleus like a giant globular cluster. Kormendy & McClure (1993) observed it with the CFHT and a camera that uses a tip-tilt mirror to partly correct seeing. At resolution $\sigma_* = 0''.18$, the limit on the core radius is $r_c < 0.39$ pc. This is as small as the smallest cores in globular clusters. The central surface brightness is one of the highest known (Figure 2). M33 is an excellent illustration of the fact that an unusually small and dense core is no evidence for a BH unless kinematic measurements show high velocities (Section 3). The central velocity dispersion measured by Kormendy & McClure (1993) is only 21 ± 3 km s^{-1}. The central mass-to-light ratio is $M/L_V \lesssim 0.4$. This is required to explain the stellar population, so a conservative limit on $M_\bullet$ is the limit on the core mass in stars: $M_\bullet \lesssim 5 \times 10^4\ M_\odot$. M33 is the first giant galaxy in which a dead quasar engine can be ruled out.

The central relaxation time, $T_r \lesssim 2 \times 10^7$ y, is so short that core collapse has probably occurred. Also, the center is $\Delta(B - R) = 0.44$ mag bluer than the rest of the nucleus. The color gradient, the F-type spectrum (van den Bergh 1991), and the small M/L ratio imply that the nucleus contains young stars concentrated to the center. Kormendy & McClure (1993) discuss the possibility that the stellar population has been affected by dynamical processes (e.g. stellar collisions).

5. GAS-DYNAMICAL BLACK HOLE SEARCHES

5.1 *M87 ($M_\bullet \simeq 3 \times 10^9\ M_\odot$)*

M87 is the father of this subject. Well known for its radio and optical jet (Biretta 1993, Macchetto 1994), it has long been the prototypical AGN galaxy in which to test the BH paradigm. It was the first giant elliptical with CCD photometry; Young et al (1978) found that it has a cuspy core. Sargent et al (1978) showed that its velocity dispersion continues to rise inside the core radius from 278 km s^{-1} at $r = 10''$ to 350 km s^{-1} at $r \simeq 1''.5$. These observations could be fitted with isotropic dynamical models only if M87 contained an MDO of mass $M_\bullet \simeq 3 \times 10^9\ M_\odot$.

But 1978 was the last year in which isotropy could be the default assumption. Illingworth (1977), Binney (1978), and others showed that most giant ellipticals are anisotropic. Models with $\sigma_r > \sigma_{\rm tangential}$ can reproduce the dispersion and

brightness profiles of M87 without an MDO (Duncan & Wheeler 1980, Binney & Mamon 1982, Richstone & Tremaine 1985, Dressler & Richstone 1990). Also, almost all giant ellipticals that are close enough to show resolved cores have profiles like that of M87 (Lauer 1985a,b; Kormendy 1985, 1987a; *HST* photometry references in Section 4.1). If cuspy cores were enough to discover black holes, we would know many examples. Similarly, if central gas and dust disks perpendicular to jets [e.g. NGC 4261 (Jaffe et al 1993)] were enough to reveal BHs, we would have many examples (Kotanyi & Ekers 1979, Kormendy & Stauffer 1987). Then this review could have been written seven years ago, and it would have been mercifully short.

The subsequent history of the BH search in M87 is reviewed by Sargent (1987), Richstone (1988), Filippenko (1988), Dressler (1989), Kormendy (1993), and van der Marel (1994a). Recently, *HST* data have revealed that $I \propto r^{-0.26}$ near the center of M87 (Lauer et al 1992a), exactly as predicted by Young et al (1978). However, this is still not sufficient evidence for a BH (Section 3). van der Marel (1994a) finds that $\sigma \simeq 400$ km s^{-1} at $r \lesssim 0\farcs5$, but he can still explain this with anisotropic models. The stellar dynamical BH case in M87 remains ambiguous.

There is hope for progress via line-of-sight velocity distributions. Black holes make broad power-law wings that extend beyond the escape velocity of the stars (van der Marel 1994a,b). But the LOSVD wings are confused with continuum variations that we do not know how to model. That is, the kinematic measurements and population synthesis are coupled. Exploiting LOSVDs will not be easy.

Gas, on the other hand, tells a clearer story. Using the second Wide Field and Planetary Camera (WFPC2) and *HST*, Ford et al (1994) have discovered that ionized nuclear gas in M87 looks like a disk with trailing spiral arms and a major axis that is perpendicular to the jet (Figure 12). Harms et al (1994) used the *HST* Faint Object Spectrograph and $0\farcs26$ diameter aperture to get spectra centered at $r = \pm 0\farcs25 = 19$ pc along the disk major axis. At a luminosity-weighted mean radius or $\pm 0\farcs22 = 16$ pc, the spectra show emission lines separated by $2V = 916$ km s^{-1}. If this gas is in circular motion and if the disk is inclined at 42° as implied by the apparent axial ratio, then M87 contains a central dark mass of $M_\bullet = 3 \times 10^9\ M_\odot$ (Table 1). This interpretion is supported by the following arguments, in decreasing order of importance. 1. Velocities at three other positions ($r = 0\farcs35, 0\farcs56$, and $2''$) agree with the Keplerian disk model. 2. At the center, the width of the emission lines is $\simeq 1700$ km s^{-1}. In fact, a large FWHM suggesting that $M_\bullet \simeq 3 \times 10^9\ M_\odot$ was already seen in ground-based data (van der Marel 1994a and references therein). 3. The disk minor axis is within 11–20° of the position angle of the jet; the inclination of the disk is $i = 42° \pm 5°$, nearly perpendicular to the jet inclination $i = -40°$ inferred by Biretta (1993). 4. Finally, spiral structure implies disk shearing.

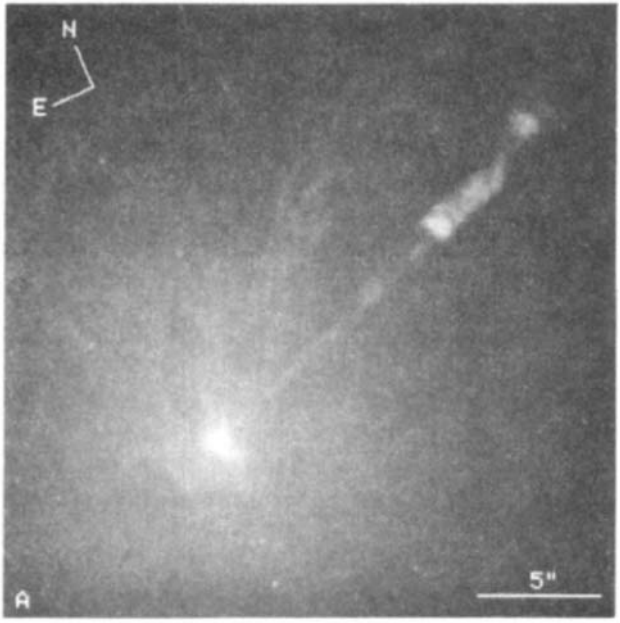

Figure 12 *HST* Hα + [N II] image of M87 (Ford et al 1994). The central ionized gas distribution is elongated perpendicular to the jet.

The caveat is that gas is easily pushed around. It may not be in circular orbits, in which case it cannot be used to measure $M_\bullet$. We emphasize that noncircular motions are not just an academic worry, they are seen in many active galaxies (e.g. Balick & Heckman 1982, Heckman et al 1993) and non-AGN environments (e.g. Fillmore et al 1986, Kormendy & Westpfahl 1989). The BH case in M87 can be strengthened (or falsified) by measuring $V(r)$ closer to the center: 0.″1 resolution is feasible, so a test for a Keplerian $V(r)$ is possible.

5.2 *NGC 4258 ($M_\bullet \simeq 4 \times 10^7\ M_\odot$)*

NGC 4258 has an AGN of modest power (Table 1) but of great interest. Its optical spectrum shows a low-ionization nuclear emission-line region (LINER) (Heckman 1980) with a weak broad-line component (Filippenko & Sargent 1985). Between its normal spiral arms, NGC 4258 has "anomalous" arms seen in Hα (Courtès & Cruvellier 1961, Deharveng & Pellet 1970), radio synchrotron emission (van der Kruit et al 1972, van Albada & van der Hulst 1982), and x rays (Pietsch et al 1994, Cecil et al 1995). The Hα arms consist of braided components (Ford et al 1986, Cecil et al 1992); the velocity field is complicated (above papers, Rubin & Graham 1990, Dettmar & Koribalski 1990). The

canonical explanation is that the nucleus emits jets in the disk plane; these interact with disk gas to produce the anomalous arm emission (above papers, Martin et al 1989, Plante et al 1991). NGC 4258 is therefore a good—albeit unusual—example of the BH paradigm.

A powerful new BH probe is provided by the detection of H_2O maser emission (Claussen et al 1984, Claussen & Lo 1986) including components ± 900 km s^{-1} from the systemic velocity (Nakai et al 1993). Greenhill et al (1995b) show that the systemic-velocity source consists of many masers along a line $0''.00026 \times 0''.00005 = 0.009 \times 0.002$ pc in extent that is perpendicular to the inner radio jet. Velocities are tightly correlated with position: $dV/dx = 270$ km s^{-1} $(0''.001)^{-1} = 7430 \pm 40$ km s^{-1} pc^{-1} along the above line. Greenhill et al (1995b), Watson & Wallin (1994), and Haschick et al (1994) suggest that the masers are in a thin annulus of radius 0.1 pc. Individual maser velocities drift by ~ 9 km s^{-1} y^{-1}, consistent with centripetal acceleration $dV/dt = V^2/r$ in the part of the annulus that is between us and the central source (Haschick et al 1994, Greenhill et al 1995a). Then the high-velocity components imply a rotation velocity of 900 km s^{-1} and a mass $M_\bullet = 2 \times 10^7 M_\odot$. These conclusions are model dependent, but they can be tested.

In an important paper, Miyoshi et al (1995) find strong evidence in favor of the disk model. With the Very Long Baseline Array, they confirm that the high-velocity masers are located $0''.005$ to $0''.008$ on either side of the central line of sources. The masing physics suggests that they radially span the edge-on torus where it is tangent to the line of sight. Then the path length to us is long at constant velocity, allowing strong maser amplification. Based on this assumption, Miyoshi et al (1995) derive the rotation curve shown in Figure 13. Remarkably, $V(r) = 2180\ (r/0''.001)^{-1/2}$ km s^{-1} $= (832 \pm 2)\ [r/(0.25\text{ pc})]^{-1/2}$ km s^{-1} is Keplerian to high precision. This is a powerful argument for the annular disk model. If the rotation is circular, then the mass interior to $0''.005 = 0.18$ pc is $M_\bullet = 4.1 \times 10^7 M_\odot$.

If Figure 13 is correct, then the $M_\bullet$ measurement is more secure than any previous one based on gas dynamics, including that of M87. This work is vulnerable on at least three counts: 1. The interpretation depends critically on the assumed geometry. The assumptions are conservative in the sense that they minimize $M_\bullet$. But the conclusion that $V \propto r^{-1/2}$ depends on the geometry, too: If the maser sources were differently distributed along the line of sight, then V could vary differently with r. Our confidence in the mass measurement depends on the Keplerian rotation curve. 2. As usual, it is not certain that gas velocities measure mass. 3. We do not know that the detected mass is dark. This work also has clear strengths: 1. The gas is molecular; being fragile, it is less likely to have noncircular velocities. 2. $V(r)$ looks Keplerian. 3. In terms of (rotation velocity)/(speed of light), the measurements get closer to the BH than in any other candidate. 4. There are no uncertainities about the

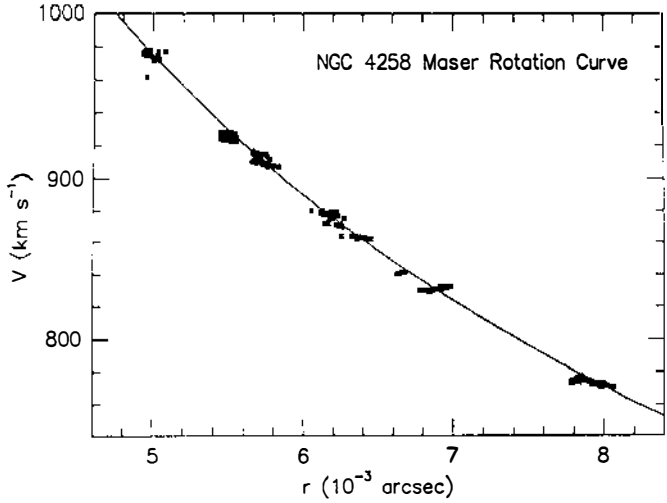

Figure 13 Rotation curve for maser sources in NGC 4258 (from Miyoshi et al 1995). The line is the Keplerian $V(r)$ given in the text.

velocity dispersion or its anisotropy. 5. The gas disk is perpendicular to the jet. 6. Finally, if $M_\bullet$ were spread out over the central 0.18 parsec, the density would be $\sim 1.6 \times 10^9\ M_\odot\ \mathrm{pc}^{-3}$. This is 70 times higher than in the Galaxy (the closest competitor). On the other hand, the *stellar* density at the Galactic center is $\sim 10^8\ M_\odot\ \mathrm{pc}^{-3}$ (Eckart et al 1993). A $1.6 \times 10^9\ M_\odot\ \mathrm{pc}^{-3}$ star cluster in not excluded, although it would evolve quickly and possibly violently.

If NGC 4258 is any indication, masers may be a powerful tool for BH searches. They allow us to probe tiny radii in great physical detail. For example, acceleration and proper motion measurements can decisively test the NGC 4258 nuclear disk model. Because masers are preferentially found in AGN galaxies (Braatz et al 1994), we can also look forward to closer connections between dynamical searches and other parts of the BH paradigm (Section 8).

6. BLACK HOLE DEMOGRAPHICS

Kormendy's CFHT BH search is being extended to 14 E–Sb galaxies with $M_B \lesssim -17.5$ and distance $\lesssim 10$ Mpc. Evidence for massive dark objects is seen in ~20% of these galaxies (M31, NGC 3115, and NGC 3377). Failures often occur where detection is unlikely because of nuclear starbursts or because the galaxy is too face-on. An example (not from the statistical sample) is NGC 1316 (Fornax A). The central dispersion is only 222 ± 4 km s^{-1} despite an unusually small and dense core (Schweizer 1980, Kormendy 1987b, Fabbiano et al 1994). The core has $M/L_V \simeq 1.5$, presumably due to an ongoing starburst

(Schweizer 1980). In such a case it is impossible to conclude anything about whether there is a BH.

It is no accident that MDOs have been found only in galaxies with favorable conditions, i.e. in edge-on bulges with rapidly rotating nuclear disks and in rotating ellipticals. Despite this, we have already found $\gtrsim 10^8\ M_\odot$ of dark matter per L^* of galaxy luminosity [where L^* is the characteristic luminosity of the Schechter (1976) luminosity function]. This is approximately the mass in dead quasars predicted by energy arguments (Sołtan 1982, Rees 1984, Chokshi & Turner 1992, Small & Blandford 1992).

With eight detections, we can start to look at demographics. If MDOs are BHs, then Figure 14 shows that BH mass correlates with bulge luminosity. The mean BH mass fraction is $\langle M_\bullet/M_{\rm bulge}\rangle = 0.0022^{+0.0016}_{-0.0009}$ (we averaged $\log M_\bullet/M_{\rm bulge}$ from Table 1). If we omit the Galaxy, which has the smallest $M_\bullet/M_{\rm bulge} = 0.00017$, then $\langle M_\bullet/M_{\rm bulge}\rangle = 0.0032^{+0.0018}_{-0.0012}$. M33 is consistent with this correlation, but also with the hypothesis that supermassive BHs are found only in bulges.

Figure 15 shows the correlations of $M_\bullet$ and $M_\bullet/M_{\rm bulge}$ with distance. It illustrates the selection effects in the search. Not surprisingly, $M_\bullet$ correlates well with distance. Giant galaxies like M87 and NGC 4594 are rare; if $M_\bullet \propto M_{\rm bulge}$, then we are unlikely to find 10^9-$M_\odot$ black holes nearby. This is why the upper-left part of the diagram is empty. On the other hand, 10^7-$M_\odot$ BHs cannot be detected very far outside the boundaries of the Local Group, at least not by stellar-dynamical searches. This ensures that the lower-right part of the diagram will remain empty until we get better spatial resolution.

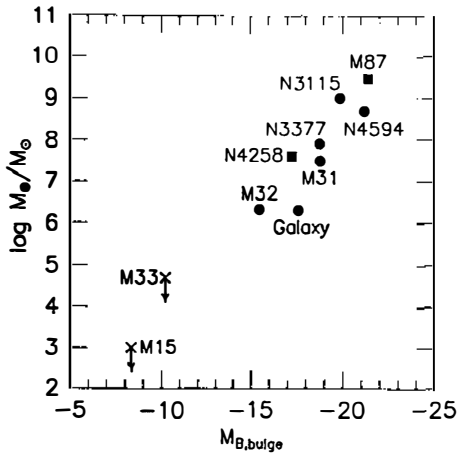

Figure 14 BH mass as a function of bulge absolute magnitude. The symbols are the same as in Figure 3. As in Figure 3, the correlation may be only the upper envelope of a distribution that extends to smaller $M_\bullet$.

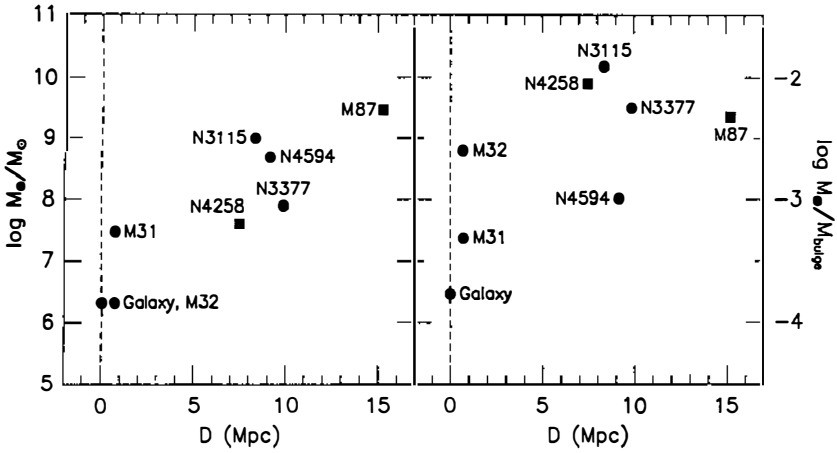

Figure 15 Correlations with distance D of detected BH mass (*left*) and BH mass divided by bulge mass (*right*).

There is little correlation of $M_\bullet/M_{\rm bulge}$ with distance D. Most BH detections were approximately equally difficult—a point also made by Rix (1993). NGC 3115 has the largest fractional BH mass and is one of the most definitive detections. M31 and the Galaxy have small fractional BH masses; a detection was possible in M31 because the nucleus rotates rapidly and in the Galaxy because the center is so nearby.

7. ARE MDOs TOO BLACK TO BE BLACK HOLES?

If massive dark objects are black holes, they should accrete nearby matter and radiate some of its binding energy. This insight provides a test for the presence of BHs.

An old stellar population produces $0.015 M_\odot\,(10^9\ L_\odot)^{-1}\ {\rm y}^{-1}$ of gas (Faber & Gallagher 1976). For example, gas shed by the bulge of M31 ($L = 6\times10^9\ L_\odot$), if accreted at a steady rate onto a BH at 10% efficiency ($\epsilon_{0.1} \equiv 1$), would provide a luminosity of $10^{11} L_\odot$. Just the stars that are gravitationally bound to the BH (i.e. at $r \lesssim 6$ pc) already generate $10^8 \epsilon_{0.1} L_\odot$. This greatly exceeds the luminosity of either nucleus.

The situation looks worse in our Galaxy. Geballe et al (1987 and references therein) estimate that IRS 16 emits a wind with velocity $v_{\rm w} \simeq 700$ km s^{-1} and mass flow rate $\sim 4\times10^{-3} M_\odot\ {\rm y}^{-1}$. If all of this matter were accreted onto a BH, its luminosity would be $10^{43}\epsilon_{0.1}$ erg s^{-1} $\simeq 10^{10}\epsilon_{0.1}\ L_\odot$. The luminosity of Sgr A* is tremendously uncertain but unlikely to be larger than 10^{40} erg s^{-1} (Genzel et al 1994a). This estimate considerably exceeds any output actually observed, but it falls short of the expected accretion luminosity

by a factor of $10^3\epsilon_{0.1}$. On the other hand, Melia (1992a, 1994) and Melia et al (1992) argue that only part of the wind is accreted, i.e. the gas that passes within $r \simeq 2GM_\bullet/v_w^2$ of the BH. Then the accretion rate is $\sim 10^{-4}$ $M_\odot\ y^{-1}$. Melia calculates the resulting spectrum; it agrees with observations over 11 decades in frequency, provided that $M_\bullet \simeq$ (1 to 2) $\times 10^6\ M_\odot$. The model has problems—it predicts a radio source size that is three times larger than the observed limit at 3 mm (Section 4.6)—but it is reasonably successful. A different model is proposed by Falcke et al (1993a,b), Falcke (1994), and Falcke & Heinrich (1995). They suggest that a dense accretion disk currently accumulates most of the above inflow; then the BH accretion rate is only 10^{-7} to $10^{-8.5}\ M_\odot\ y^{-1}$. However, their disk radiates more efficiently, so it also fits the observed spectrum. Similar models fit M31 (Melia 1992b, Falcke & Heinrich 1995). So: The accretion physics is still under discussion, but there is no clear luminosity problem.

The Falcke model illustrates the easy escape from any BH luminosity problem: We can hypothesize nonsteady accretion. It is possible that normal nuclei cycle between an accreting, low-level AGN state and a nonaccreting, normal state.

A second fuel source for nuclear BHs is accretion of stars (e.g. Lacy et al 1982; Rees 1988; Goodman & Lee 1989; Phinney 1989; Evans & Kochanek 1989; Rees 1990, 1993, 1994). A BH will tidally disrupt main-sequence stars on relativistic orbits. For sufficiently low-mass BHs, tidal disruption occurs outside the Schwarzschild radius. Half of the stellar mass is likely to be accreted, with an energy output of $10^{53}\ m_*\ \epsilon_{0.1}$ erg. Stars that are initially on doomed orbits will be destroyed within an orbital timescale of the formation of the BH. Later, stars are destroyed at the rate at which these orbits are repopulated.

The rate of repopulation of the "loss cone" (actually more nearly a cylinder) by two-body gravitational interactions is a well-studied but very complicated subject originally motivated by the expectation that BHs form in globular clusters. There are two regimes: 1. Sufficiently close to the hole, stars scatter into or out of the loss cone on timescales that are longer than the orbital time. Stars scattered into the cone die almost instantaneously and the cone is empty. In this case, the calculation of the disruption rate is complicated by the necessity to treat this empty part of phase space as a boundary condition on the evolution of the phase space density of stars. 2. Farther from the hole, the timescale for small changes in rms angular momentum is short compared to an orbital time; the loss cone is therefore populated. Estimates of stellar disruption are complicated by the likelihood that stars will scatter out of the loss cone before reaching the perilous environs of the BH. In either case, it is clear on dimensional grounds that the stellar destruction rate is bounded from above by $dN/dt = N/t_r$, where t_r is the half-mass relaxation time and N is the number of stars bound to the BH (that is, with $r < r_{cusp} \equiv GM_\bullet/\sigma^2$). Improving on

this limit is difficult. The reader is referred to a very lucid review by Shapiro (1985) and to Cohn & Kulsrud (1978), particularly their equation 66:

$$\frac{dN}{dt} = 0.018 M_8^{2.33} n_4^{1.60} \left[\frac{\sigma^2}{(100\ \mathrm{km\ s^{-1}})^2}\right]^{-2.88} m_*^{1.06} r_*^{0.40}\ \mathrm{y}^{-1}. \quad (3)$$

Here $M_8 = M_\bullet/(10^8 M_\odot)$, n_4 is the stellar density at the cusp radius $r_{\rm cusp}$ in units of 10^4 pc^{-3}, and m_* and r_* are the typical stellar mass and radius, respectively, in solar units.

Applying these equations to M31, for $M_8 = 0.3$ (Table 1), $r_{\rm cusp} \simeq 6$ pc, and $n_4 = 1$ (Lauer et al 1993), we find a stellar disruption rate of 10^{-4} y^{-1}. This is consistent with results in Rees (1988) and in Goodman & Lee (1989). What happens to the shattered star? Tidal breakup occurs at a radius $r_t = 2.3 \times 10^{13} M_8^{1/3} m_*^{-1/3} r_*$ cm. The Schwarzschild radius of the BH is $r_S = 3.0 \times 10^{13} M_8$ cm. So for $M_8 < 1$, solar-mass main-sequence stars are disrupted outside the Schwarzschild radius and the fireworks should be visible. Note that the rate of breakup flashes could be greatly enhanced over the above estimate by the accretion of a second BH or even of a secondary nucleus. One or both of these things may be happening in M31, so the current rate of stellar breakup flashes could be much larger than the above estimate.

The least certain aspects of this problem are the duration and spectrum of a flash. The stream of bound debris from the shattered star will self-intersect within months. The gas should shock and transfer angular momentum efficiently. Rapid relativistic perhelion precession probably precludes the formation of an elliptical disk, so the timescale for the event is likely to be $\lesssim$1 y. On the other hand, Cannizzo et al (1990) note that at late times there is a self-similar disk accretion solution that may preserve a power-law decay for many years. If they are correct, then the inactivity of M31 is a serious argument against a nuclear BH.

We are unaware of any calculation of the spectrum of the flashes. If the debris forms dust rapidly and becomes optically thick, then the radiation will be reprocessed in a region significantly larger than r_t, and most of the signal will emerge in the infrared (as emphasized by Rees, personal communication). If, on the other hand, the stellar orbital angular momentum is aligned with that of the BH, or if the BH has negligible angular momentum, then the debris may orbit in a plane and the luminosity might be dominated by the inner edge of the accretion disk. Then the temperature could be near 500,000 K and the resulting spectrum would peak in the extreme ultraviolet or soft x-ray band (Sembay & West 1993). Given a large sample with diverse angular momentum alignments, soft x-ray and infrared flashes both probably occur.

If one considers the possibly short duty cycle and its uncertainties, the absence of activity in M31 or in any other BH candidate is not terribly disturbing. Some low-level AGNs noted by Filippenko & Sargent (1985, 1987) may even

be powered by stellar breakup flashes. A key test of the BH paradigm is nevertheless implied. A survey of 10^4 galaxies should yield one stellar breakup flash per year at luminosities exceeding those of supernovae. Periodic imaging of a set of clusters of galaxies should be informative very quickly (Rees 1994). It is even possible that several hundred x-ray flashes have already been detected by the *ROSAT* all-sky survey (Sembay & West 1993).

8. CONCLUSION

Have we discovered BHs in galaxy nuclei? Rigorously, we have not. Dynamical proof requires measurement of relativistic velocities near the Schwarzschild radius, $r_S \simeq 2M_8$ AU $\simeq M_8 \times 10^{-5}$ pc. Even for M31, this is 3×10^{-6} arcsec. *HST* spectroscopic resolution is only 0".1. What dynamical searches have contributed is the first solid evidence for massive dark objects in galaxy nuclei. In Section 2, we called this step 1 of the BH search. The dynamics also show that $M_\bullet$ is in the range expected for quasar engines, and they tell us a little about MDO demographics. Are MDOs BHs? The arguments are inconclusive. Steps 2 and 3—proof that MDOs are (or are not) BHs and the study of BH statistics—are barely begun.

If the BH picture is compelling, it is because of the combination of dynamical searches and AGN evidence. A review of AGNs is beyond the scope of this paper, but it is useful to recall the observations that point most directly to BHs. (*a*) Superluminal jets show that AGN engines are relativistically compact. (*b*) AGN engines remember jet ejection directions for a long time, suggesting that they are good gyroscopes. (*c*) Rapid time variability and very-long-baseline interferometry show that AGN engines are tiny. (*d*) The prodigious energy output of quasars requires that AGN engines be very efficient.

These are also the strongest arguments against the best alternative to the black hole picture: that AGNs are powered by starbursts (e.g. Terlevich & Melnick 1985; Terlevich et al 1987, 1993; Filippenko 1989, 1991, 1992b, 1993; Heckman 1991; Terlevich 1992; Tenorio-Tagle et al 1992; Terlevich & Boyle 1993; meetings devoted to this subject include Filippenko 1992a, Beckman et al 1993). It is difficult to imagine that a starburst can produce a superluminal jet or a jet that stays collimated over a Mpc. Something like a BH is required even if AGNs are partly powered by starbursts. In addition, starburst energy conversion efficiencies are a factor of ~ 10 lower than those of BHs, so the starburst model predicts MDO masses of $\gtrsim 10^{10}\, M_\odot$ for dead quasars. If such massive MDOs existed within 15 Mpc of us, we would not be struggling to find them. Other arguments against the extreme starburst hypothesis are given in Heckman (1995). However, no observation conflicts with the idea that starbursts play a role in quasar formation (Sanders et al 1988a,b), and it is possible that some low-level AGNs are powered entirely by starbursts (see the above references, Filippenko et al 1993). Meanwhile, AGN observations

and theory, and now the results of the dynamical searches, make a compelling picture in favor of the BH paradigm.

Still, we cannot help but note that this rosy picture is not developing as a correct paradigm should. The dynamical searches and AGN results have remained almost decoupled. The galaxies with stellar-dynamical evidence for BHs are spectacularly inactive. Table 1 lists nuclear radio continuum fluxes. M31 contains the lowest-luminosity radio AGN known (Crane et al 1992, 1993a). Sgr A* and M32 are comparably weak. Because of its inactivity, NGC 3115 has been used as an emission-line-less spectral standard in searches for low-level AGNs (Filippenko & Sargent 1985, Ho et al 1993). Among stellar-dynamical BH cases, only NGC 4594 is somewhat active. It contains a LINER (Heckman 1980), i.e. a dwarf Seyfert 1 nucleus of Hα width at zero intensity ~ 5400 km s^{-1} (Filippenko & Sargent 1985, 1987). But NGC 4594 is an order of magnitude lower in radio luminosity than M87. Even M87 is a weak radio galaxy. In contrast, many AGNs that are no farther away show no dynamical evidence for BHs. To be sure, as A Dressler (personal communication) has said, BHs are not easily discovered when we have a searchlight in our eyes. Also, there is every reason to expect dead AGNs all around us. But our confidence is not helped by the fact that galaxies with MDOs are so inactive while AGN BHs are so elusive.

This is why the M87 and NGC 4258 results (Section 5) are so welcome. M87 epitomizes the AGN paradigm. Now the detection of a nuclear gas disk perpendicular to the jet and with velocities implying a BH of just the right mass is the first direct contact between BH searches and the rest of the paradigm. It will be important to check whether the disk is in Keplerian rotation and hence whether the velocities measure mass, but the apparent detection of a Keplerian rotation curve in NGC 4258 already increases our confidence in gas-dynamical BH searches.

Which leads us to our "top ten" wish list:

1. We need to address any lingering doubts about the best BH cases. This requires at least one iteration in improved spatial resolution over the discovery observations plus dynamical models that explore the boundaries between extreme models with constant M/L and ones that contain BHs.

2. Theory may help us to eliminate some models. Reducing M/L requires radial anisotropy; such models may be unstable (e.g. Merritt 1987, Stiavelli et al 1993, Bertin et al 1994, and references therein).

3. Shortcuts for the identification of BH candidates would be helpful. For example, Kormendy (1992a,b, 1993) showed that BH candidates deviate from the core fundamental plane correlations: They have large apparent central velocity dispersions for their core parameters.

4. Further work on emission-line velocity fields is promising.

5. Our ultimate goal is to understand BH demographics. At a minimum, we want to know the frequency of occurrence and mass function of BHs as a function of Hubble type. This will be expensive.

6. Surely the most fundamental challenge is to show whether or not MDOs are BHs. Our observations are 10^5 Schwarzschild radii away from the action. The obvious way to get closer is to look at more energetic photons. One possibility is to use x-ray spectroscopy. But gas will always be responsive, and gas dynamical searches will always be uncertain.

   This issue is important. Even if AGNs are not *primarily* starbursts, starbursts happen, and Terlevich and collaborators correctly point out that they leave remnants. In detecting MDOs, could we just be finding those dead star clusters? In fact, given our present ignorance, can we even be sure that MDOs are not concentrations of halo dark matter?

7. Therefore, work on alternatives to the BH paradigm is still desirable.

8. How did black holes form? Kormendy (1988b) points out that core relaxation times are almost everywhere so long that BH formation via dynamical evolution (e.g. core collapse) seems impossible. Rees (1984) suggests formation mechanisms that do not depend on relaxation; we do not know which (if any) are correct. The problem is particularly acute because quasars turned on so early in the history of the Universe: BHs must have formed quickly (e.g. Rees 1990, 1993). As long as BH formation remains obscure, we have a glaring hole in the AGN paradigm.

9. Should MDOs be so inactive? Predictions of flaring frequencies (Section 7) may lead to tests of the BH picture.

10. More generally, we need to look for points of contact between dynamical BH searches and the AGN paradigm. Confidence and progress both are at stake.

This review is being written at a time of unusually rapid progress. We have discussed ongoing work as much as possible. But stay tuned: By the time this paper appears, *HST* should begin to provide stellar-dynamical results on the most important BH candidates.

ACKNOWLEDGMENTS

It is a pleasure to thank the many people who sent preprints and reprints, including those on subjects that were not covered because of space limitations. We also thank R Bender, A Evans, S Faber, R Genzel, F Melia, J Moran, G

Rieke, S Tremaine, and R van der Marel for helpful discussions or permission to quote results before publication. We are grateful to the following for providing figures or data for figures: S Faber (data for Figure 3), T Lauer (Figure 4), A Dressler (data for Figure 5), R Bacon and G Monnet (Figure 6), R Bender (LOSVDs in Figure 7), W Dehnen and R van der Marel (who calculated their M32 models as seen at SIS resolution, Figure 10), R Genzel (Figure 11), H Ford (Figure 12), and J Moran (data for Figure 13). Our own work on the BH search benefits enormously from efforts at the CFHT to improve the image quality. JK's work has been supported by NSF grants AST 8915021 and AST 9219221. DR is supported by NASA grant NAG 5-2758. This paper has made use of the NASA/IPAC Extragalactic Database (NED), which is operated by JPL and Caltech under contract with NASA.

Literature Cited

Allen DA. 1994. See Genzel & Harris 1994, p. 293
Bacon R, Emsellem E, Monnet G, Nieto J-L. 1994. *Astron. Astrophys.* 281:691
Backer DC, ed. 1987. *The Galactic Center.* New York: Am. Inst. Phys.
Bahcall JN, Wolf RA. 1976. *Ap. J.* 209:214
Balick B, Heckman TM. 1982. *Annu. Rev. Astron. Astrophys.* 20:431
Beckman J, Colina L, Netzer H, eds. 1993. *The Nearest Active Galaxies.* Madrid: Cons. Super. Invest. Científicas
Begelman MC, Blandford RD, Rees MJ. 1984. *Rev. Mod. Phys.* 56:255
Bender R. 1990. *Astron. Astrophys.* 229:441
Bender R, Burstein D, Faber SM. 1992. *Ap. J.* 399:462
Bender R, Burstein D, Faber SM. 1993. *Ap. J.* 411:153
Bender R, Saglia RP, Gerhard OE. 1994. *MNRAS* 269:785
Bertin G, Pegoraro F, Rubini F, Vesperini E. 1994. *Ap. J.* 434:94
Binney J. 1978. *MNRAS* 183:501
Binney J. 1980. *MNRAS* 190:873
Binney J, Mamon GA. 1982. *MNRAS* 200:361
Biretta JA. 1993. In *Astrophysical Jets,* ed. D Burgarella, M Livio, C O'Dea, p. 263. Cambridge: Cambridge Univ. Press
Biretta JA, Owen FN, Hardee PE. 1983. *Ap. J. Lett.* 274:L27
Blandford RD. 1990. In *Active Galactic Nuclei, Saas-Fee Advanced Course 20,* ed. TJ-L Courvoisier, M Mayor, p. 161. Berlin: Springer-Verlag
Blandford RD, Rees MJ. 1992. In *Testing the AGN Paradigm,* ed. SS Holt, SG Neff, CM Urry, p. 3. New York: Am. Inst. Phys.
Bower GA, Richstone DO, Bothun GD, Heckman TM. 1993. *Ap. J.* 402:76
Braatz JA, Wilson AS, Henkel C. 1994. *Ap. J. Lett.* 437:L99
Burkhead MS. 1986. *Astron. J.* 91:777
Burkhead MS. 1991. *Astron. J.* 102:893
Burstein D, Heiles C. 1984. *Ap. J. Suppl.* 54:33
Cannizzo JK, Lee HM, Goodman J. 1990. *Ap. J.* 351:38
Capaccioli M, Held EV, Nieto J-L. 1987. *Astron. J.* 94:1519
Carter D, Jenkins CR. 1993. *MNRAS* 263:1049
Cecil G, Wilson AS, De Pree C. 1995. *Ap. J.* 440:181
Cecil G, Wilson AS, Tully RB. 1992. *Ap. J.* 390:365
Chokshi A, Turner EL. 1992. *MNRAS* 259:421
Claussen MJ, Heiligman GM, Lo KY. 1984. *Nature* 310:298
Claussen MJ, Lo K-Y. 1986. *Ap. J.* 308:592
Cohn H, Kulsrud RM. 1978. *Ap. J.* 226:1087
Courtès G, Cruvellier P. 1961. *C. R. Acad. Sci. Paris* 253:218
Crane PC, Cowan JJ, Dickel JR, Roberts DA. 1993a. *Ap. J. Lett.* 417:L61
Crane PC, Dickel JR, Cowan JJ. 1992. *Ap. J. Lett.* 390:L9
Crane P, Stiavelli M, King IR, Deharveng JM, Albrecht R, et al. 1993b. *Astron. J.* 106:1371
Davies RL. 1989. In *The World of Galaxies,* ed. HG Corwin, L Bottinelli, p. 312. Berlin: Springer-Verlag

Davies RL, Efstathiou G, Fall SM, Illingworth G, Schechter PL. 1983. *Ap. J.* 266:41
de Bruyn AG, Crane PC, Price RM, Carlson JB. 1976. *Astron. Astrophys.* 46:243
Deharveng JM, Pellet A. 1970. *Astron. Astrophys.* 9:181
Dehnen W. 1993. *MNRAS* 265:250
Dehnen W. 1995. *MNRAS* In press
Dehnen W, Gerhard OE. 1993. *MNRAS* 261:311
Dehnen W, Gerhard OE. 1994. *MNRAS* 268:1019
Dettmar R-J, Koribalski B. 1990. *Astron. Astrophys.* 240:L15
de Vaucouleurs G. 1958. *Ap. J.* 128:465
de Vaucouleurs G, de Vaucouleurs A, Corwin HG, Buta RJ, Paturel G, Fouqué P. 1991. *Third Reference Catalogue of Bright Galaxies.* Berlin: Springer-Verlag
de Vaucouleurs G, Pence WD. 1978. *Astron. J.* 83:1163
de Zeeuw T. 1993. In *IAU Symp. 153, Galactic Bulges,* ed. H Dejonghe, HJ Habing, p. 191. Dordrecht: Kluwer
de Zeeuw PT. 1994. In *The Formation and Evolution of Galaxies,* ed. C. Muñoz-Tuñón, F Sánchez, p. 231. Cambridge: Cambridge Univ. Press.
Djorgovski S, de Carvalho R, Han M-S. 1988. In *The Extragalactic Distance Scale,* ed. S van den Bergh, CJ Pritchet, p. 329. San Francisco: Astron. Soc. Pac.
Dressler A. 1984. *Ap. J.* 286:97
Dressler A. 1989. In *IAU Symp. 134, Active Galactic Nuclei,* ed. DE Osterbrock, JS Miller, p. 217. Dordrecht: Kluwer
Dressler A, Richstone DO. 1988. *Ap. J.* 324:701
Dressler A, Richstone DO. 1990. *Ap. J.* 348:120
Dubath P, Meylan G. 1994. *Astron. Astrophys.* 290:104
Dubath P, Meylan G, Mayor M. 1994. *Ap. J.* 426:192
Duncan MJ, Wheeler JC. 1980. *Ap. J. Lett.* 237:L27
Eckart A, Genzel R, Hofmann R, Sams BJ, Tacconi-Garman LE, et al. 1994. See Genzel & Harris 1994, p. 305
Eckart A, Genzel R, Krabbe A, Hofmann R, van der Werf PP, Drapatz S. 1992. *Nature* 355:526
Eckart A, Genzel R, Hofmann R, Sams BJ, Tacconi-Garman LE. 1993. *Ap. J. Lett.* 407:L77
Emsellem E, Bacon R, Monnet G. 1994b. In *IAU Colloq. 149, Tridimensional Optical Spectroscopic Methods in Astrophysics,* ed. G Compte, M Marcelin, p. 282. San Francisco: Astron. Soc. Pac.
Emsellem E, Monnet G, Bacon R, Nieto J-L. 1994a. *Astron. Astrophys.* 285:739
Evans CR, Kochanek CS. 1989. *Ap. J. Lett.* 346:L13
Evans NW, de Zeeuw PT. 1994. *MNRAS* 271:202
Fabbiano G, Fassnacht C, Trinchieri G. 1994. *Ap. J.* 434:67
Fabbiano G, Gioia IM, Trinchieri G. 1989. *Ap. J.* 347:127
Fabbiano G, Klein U, Trinchieri G, Wielebinski R. 1987. *Ap. J.* 312:111
Faber SM. 1973. *Ap. J.* 179:731
Faber SM, Dressler A, Davies RL, Burstein D, Lynden-Bell D, et al. 1987. In *Nearly Normal Galaxies: From the Planck Time to the Present,* ed. SM Faber, p. 175. Berlin: Springer-Verlag
Faber SM, Gallagher JS. 1976. *Ap. J.* 204:365
Faber SM, Kormendy J, Ajhar EA, Byun Y-I, Dressler A, et al. 1995. *Astron. J.* In prep.
Faber SM, Wegner G, Burstein D, Davies RL, Dressler A, et al. 1989. *Ap. J. Suppl.* 69:763
Faber SM, Worthey G, Gonzalez JJ. 1992. In *IAU Symp. 149, The Stellar Populations of Galaxies,* ed. B Barbuy, A Renzini, p. 255. Dordrecht: Kluwer
Falcke H. 1994. In *IAU Symp. 169, Unsolved Problems of the Milky Way,* ed. L Blitz. Dordrecht: Kluwer. In press
Falcke H, Biermann PL, Duschl WJ, Mezger PG. 1993a. *Astron. Astrophys.* 270:102
Falcke H, Heinrich OM. 1995. *Astron. Astrophys.* In press
Falcke H, Mannheim K, Biermann PL. 1993b. *Astron. Astrophys.* 278:L1
Ferrarese L, van den Bosch FC, Ford HC, Jaffe W, O'Connell RW. 1994. *Astron. J.* 108:1598
Filippenko AV. 1988. See Kafatos 1988, p. 104
Filippenko AV. 1989. In *IAU Symp. 134, Active Galactic Nuclei,* ed. DE Osterbrock, JS Miller, p. 495. Dordrecht: Kluwer
Filippenko AV. 1991. In *Physics of Active Galactic Nuclei,* ed. WJ Duschl, SJ Wagner, p. 345. Berlin: Springer-Verlag
Filippenko AV, ed. 1992a. *Relationships Between Active Galactic Nuclei and Starburst Galaxies.* San Francisco: Astron. Soc. Pac.
Filippenko AV. 1992b. See Filippenko 1992a, p. 253
Filippenko AV. 1993. See Beckman et al 1993, p. 99
Filippenko AV, Conti PS, Genzel R, Heckman TM, Mushotzky RF, Terlevich RJ. 1993. See Beckman et al 1993, p. 257
Filippenko AV, Sargent WLW. 1985. *Ap. J. Suppl.* 57:503
Filippenko AV, Sargent WLW. 1987. In *IAU Symp. 121, Observational Evidence of Activity in Galaxies,* ed. E Ye Khachikian, KJ Fricke, J Melnick, p. 451. Dordrecht: Reidel
Fillmore JA, Boroson TA, Dressler A. 1986. *Ap. J.* 302:208
Forbes DA. 1994. *Astron. J.* 107:2017
Forbes DA, Franx M, Illingworth GD. 1994. *Ap. J. Lett.* 428:L49
Ford HC, Dahari O, Jacoby GH, Crane PC, Ciardullo R. 1986. *Ap. J. Lett.* 311:L7
Ford HC, Harms RJ, Tsvetanov ZI, Hartig GF, Dressel LL, et al. 1994. *Ap. J. Lett.* 435:L27

Geballe TR, Wade R, Krisciunas K, Gatley I, Bird MC. 1987. *Ap. J.* 320:562
Genzel R, Harris AI, eds. 1994. *The Nuclei of Normal Galaxies: Lessons from the Galactic Center.* Dordrecht: Kluwer
Genzel R, Hollenbach D, Townes CH. 1994a. *Rep. Prog. Phys.* 57:417
Genzel R, Hollenbach DJ, Townes CH, Eckart A, Krabbe A, et al. 1994b. See Genzel & Harris 1994, p. 327
Genzel R, Townes CH. 1987. *Annu. Rev. Astron. Astrophys.* 25:377
Gerhard OE. 1988. *MNRAS* 232:13P
Gerhard OE. 1989. In *Dynamics of Dense Stellar Systems,* ed. D Merritt, p. 61. Cambridge: Cambridge Univ. Press
Gerhard OE. 1991. *MNRAS* 250:812
Gerhard OE. 1992. In *Physics of Active Galactic Nuclei,* ed. WJ Duschl, SJ Wagner, p. 273. Berlin: Springer-Verlag
Gerhard OE. 1993a. In *ESO/EIPC Workshop on the Structure, Dynamics, and Chemical Evolution of Elliptical Galaxies,* ed. IJ Danziger, WW Zeilinger, K Kjär, p. 311. Munich: ESO
Gerhard OE. 1993b. *MNRAS* 265:213
Goodman J, Lee HM. 1989. *Ap. J.* 337:84
Greenhill LJ, Henkel C, Becker R, Wilson TL, Wouterloot JGA. 1995a. *Astron. Astrophys.* In press
Greenhill LJ, Jiang DR, Moran JM, Reid MJ, Lo KY, Claussen MJ. 1995b. *Ap. J.* 440:619
Haller JW, Rieke MJ, Rieke GH, Tamblyn P, Close L, et al. 1995. *Ap. J.* In prep.
Harms RJ, Ford HC, Tsvetanov ZI, Hartig GF, Dressel LL, et al. 1994. *Ap. J. Lett.* 435:L35
Haschick AD, Baan WA, Peng EW. 1994. *Ap. J. Lett.* 437:L35
Heckman TM. 1980. *Astron. Astrophys.* 87:152
Heckman TM. 1991. In *Massive Stars in Starbursts,* ed. C Leitherer, NR Walborn, TM Heckman, CA Norman, p. 289. Cambridge: Cambridge Univ. Press
Heckman TM. 1995. In *Mass-Transfer-Induced Activity in Galaxies.* 274:602
Heckman TM, Lehnert MD, Armus L. 1993. See Beckman et al 1993, p. 133
Ho LC, Filippenko AV, Sargent WLW. 1993. *Ap. J.* 417:63
Hummel E. 1980. *Astron. Astrophys. Suppl.* 41:151
Hunter C, Qian E. 1993. *MNRAS* 262:401
Illingworth G. 1977. *Ap. J. Lett.* 218:L43
Illingworth G, Schechter PL. 1982. *Ap. J.* 256:481
Jaffe W, Ford HC, Ferrarese L, van den Bosch F, O'Connell RW. 1993. *Nature* 364:213
Jarvis BJ, Dubath P. 1988. *Astron. Astrophys.* 201:L33
Jarvis BJ, Freeman KC. 1985. *Ap. J.* 295:324
Johnson HM. 1961. *Ap. J.* 133:309
Kafatos M, ed. 1988. *Supermassive Black Holes.* Cambridge: Cambridge Univ. Press
Kent SM. 1987a. *Astron. J.* 93:816
Kent SM. 1987b. *Astron. J.* 94:306
Kent SM. 1992. *Ap. J.* 387:181
Kent SM, Dame TM, Fazio G. 1991. *Ap. J.* 378:131
King IR, Stanford SA, Crane P. 1995. *Astron. J.* 109:164
Kinman TD. 1965. *Ap. J.* 142:1376
Kormendy J. 1982. In *Morphology and Dynamics of Galaxies, 12th Adv. Course Swiss Soc. Astron. Astrophys.,* ed. L Martinet, M Mayor, p. 113. Sauverny: Geneva Obs.
Kormendy J. 1983. *Ap. J.* 275:529
Kormendy J. 1985. *Ap. J. Lett.* 292:L9
Kormendy J. 1987a. In *IAU Symp. 127, Structure and Dynamics of Elliptical Galaxies,* ed. T de Zeeuw, p. 17. Dordrecht: Reidel
Kormendy J. 1987b. In *Nearly Normal Galaxies: From the Planck Time to the Present,* ed. SM Faber, p. 163. Berlin: Springer-Verlag
Kormendy J. 1988a. See Kafatos 1988, p. 98
Kormendy J. 1988b. See Kafatos 1988, p. 219
Kormendy J. 1988c. *Ap. J.* 325:128
Kormendy J. 1988d. *Ap. J.* 335:40
Kormendy J. 1989. *Ap. J. Lett.* 342:L63
Kormendy J. 1992a. In *Testing the AGN Paradigm,* ed. SS Holt, SG Neff, CM Urry, p. 23. New York: Am. Inst. Phys.
Kormendy J. 1992b. In *High Energy Neutrino Astrophysics,* ed. VJ Stenger, JG Learned, S Pakvasa, X Tata, p. 196. Singapore: World Scientific
Kormendy J. 1993. See Beckman et al 1993, p. 197
Kormendy J. 1994. See Genzel & Harris 1994, p. 379
Kormendy J, et al. 1995a. *Astron. J.* To be published
Kormendy J, Bender R. 1995. *Astron. J.* In prep.
Kormendy J, Djorgovski S. 1989. *Annu. Rev. Astron. Astrophys.* 27:235
Kormendy J, Dressler A, Byun Y-I, Faber SM, Grillmair C, et al. 1994. In *ESO/OHP Workshop on Dwarf Galaxies,* ed. G Meylan, P Prugniel, p. 147. Garching: ESO
Kormendy J, Evans AS, Richstone D. 1995b. In prep.
Kormendy J, Illingworth G. 1982. *Ap. J.* 256:460
Kormendy J, McClure RD. 1993. *Astron. J.* 105:1793
Kormendy J, Richstone D. 1992. *Ap. J.* 393:559 (KR92)
Kormendy J, Stauffer J. 1987. In *IAU Symp. 127, Structure and Dynamics of Elliptical Galaxies,* ed. T de Zeeuw, p. 405. Dordrecht: Reidel
Kormendy J, Westpfahl DJ. 1989. *Ap. J.* 338:752
Kotanyi CG, Ekers RD. 1979. *Astron. Astrophys.* 73:L1
Krabbe A, Genzel R, Eckart A, Najarro F, Lutz D, et al. 1995. *Ap. J. Lett.* Submitted
Krause M, Cox P, Garcia-Barreto JA, Downes D. 1990. *Astron. Astrophys.* 233:L1
Kuijken K, Merrifield MR. 1993. *MNRAS* 264:712

Lacy JH, Townes CH, Hollenbach DJ. 1982. *Ap. J.* 262:120
Lallemand A, Duchesne M, Walker MF. 1960. *Publ. Astron. Soc. Pac.* 72:76
Lauer TR. 1985a. *Ap. J. Suppl.* 57:473
Lauer TR. 1985b. *Ap. J.* 292:104
Lauer TR, Ajhar EA, Byun Y-I, Dressler A, Faber SM, et al. 1995. *Astron. J.* Submitted
Lauer TR, Faber SM, Currie DG, Ewald SP, Groth EJ, et al. 1992b. *Astron. J.* 104:552
Lauer TR, Faber SM, Groth EJ, Shaya EJ, Campbell B, et al. 1993. *Astron. J.* 106:1436
Lauer TR, Faber SM, Holtzman JA, Baum WA, Currie DG, et al. 1991a. *Ap. J. Lett.* 369:L41
Lauer TR, Faber SM, Lynds CR, Baum WA, Ewald SP, et al. 1992a. *Astron. J.* 103:703
Lauer TR, Holtzman JA, Faber SM, Baum WA, Currie DG, et al. 1991b. *Ap. J. Lett.* 369:L45
Light ES, Danielson RE, Schwarzschild M. 1974. *Ap. J.* 194:257
Lindqvist M, Habing HJ, Winnberg A. 1992. *Astron. Astrophys.* 259:118
Lo KY, Backer DC, Ekers RD, Kellermann KI, Reid M, Moran JM. 1985. *Nature* 315:124
Lucy LB. 1974. *Astron. J.* 79:745
Lynden-Bell D. 1969. *Nature* 223:690
Lynden-Bell D. 1978. *Phys. Scr.* 17:185
Lynden-Bell D, Faber SM, Burstein D, Davies RL, Dressler A, et al. 1988. *Ap. J.* 326:19
Lynden-Bell D, Rees MJ. 1971. *MNRAS* 152:461
Macchetto F. 1994. In *IAU Symp. 159, Multi-Wavelength Continuum Emission of AGN,* ed. T J-L Courvoisier, A Blecha, p. 83. Dordrecht: Kluwer
Martin P, Roy J-R, Noreau L, Lo KY. 1989. *Ap. J.* 345:707
McGinn MT, Sellgren K, Becklin EE, Hall DNB. 1989. *Ap. J.* 338:824
Melia F. 1992a. *Ap. J. Lett.* 387:L25
Melia F. 1992b. *Ap. J. Lett.* 398:L95
Melia F. 1994. *Ap. J.* 426:577
Melia F, Jokipii JR, Narayanan A. 1992. *Ap. J. Lett.* 395:L87
Merritt D. 1987. *Ap. J.* 319:55
Meylan G, Pryor C. 1993. In *Structure and Dynamics of Globular Clusters,* ed. SG Djorgovski, G Meylan, p. 31. San Francisco: Astron. Soc. Pac.
Mirabel IF, Rodríguez LF, Cordier B, Paul J, Lebrun F. 1992. *Nature* 358:215
Miyoshi M, Moran J, Herrnstein J, Greenhill L, Nakai N, et al. 1995. *Nature* 373:127
Morris M, ed. 1989. *IAU Symp. 136, The Center of Our Galaxy.* Dordrecht: Kluwer
Morris M. 1993. In *Back to the Galaxy,* ed. SS Holt, F Verter, p. 21. New York: Am. Inst. Phys.
Nakai N, Inoue M, Miyoshi M. 1993. *Nature* 361:45
Newell B, Da Costa GS, Norris J. 1976. *Ap. J. Lett.* 208:L55
Pais A. 1986. *Inward Bound: Of Matter and Forces in the Physical World.* New York: Oxford Univ. Press
Peebles PJE. 1972. *Ap. J.* 178:371
Peterson RC, Seitzer P, Cudworth KM. 1989. *Ap. J.* 347:251
Phinney ES. 1989. See Morris 1989, p. 543
Pietsch W, Vogler A, Kahabka P, Jain A, Klein U. 1994. *Astron. Astrophys.* 284:386
Plante RL, Lo KY, Roy J-R, Martin P, Noreau L. 1991. *Ap. J.* 381:110
Qian EE, de Zeeuw PT, van der Marel RP, Hunter C. 1995. *MNRAS* 274:602
Rees MJ. 1984. *Annu. Rev. Astron. Astrophys.* 22:471
Rees MJ. 1987. See Backer 1987, p. 71
Rees MJ. 1988. *Nature* 333:523
Rees MJ. 1990. *Science* 247:817
Rees MJ. 1993. *Proc. Natl. Acad. Sci.* 90:4840
Rees MJ. 1994. See Genzel & Harris 1994, p. 453
Richardson WH. 1972. *J. Opt. Soc. Am.* 62:52
Richstone DO. 1988. See Kafatos 1988, p. 87
Richstone D. 1993. In *Texas/Pascos '92: Relativistic Astrophysics and Particle Cosmology,* ed. CW Akerlof, MA Srednicki, p. 716. New York: NY Acad. Sci.
Richstone D, Bower G, Dressler A. 1990. *Ap. J.* 353:118
Richstone DO, Tremaine S. 1984. *Ap. J.* 286:27
Richstone DO, Tremaine S. 1985. *Ap. J.* 296:370
Richstone DO, Tremaine S. 1988. *Ap. J.* 327:82
Rieke GH, Rieke MJ. 1988. *Ap. J. Lett.* 330:L33
Rieke GH, Rieke MJ. 1994. See Genzel & Harris 1994, p. 283
Rix H-W. 1993. In *IAU Symp. 153, Galactic Bulges,* ed. H Dejonghe, HJ Habing, p. 423. Dordrecht: Kluwer
Rix H-W, White SDM. 1992. *MNRAS* 254:389
Rogers AEE, Doeleman S, Wright MCH, Bower GC, Backer DC, et al. 1994. *Ap. J. Lett.* 434:L59
Rubin VC, Graham JA. 1990. *Ap. J. Lett.* 362:L5
Saha P, Williams TB. 1994. *Astron. J.* 107:1295
Salpeter EE. 1964. *Ap. J.* 140:796
Sandage A. 1961. *The Hubble Atlas of Galaxies.* Washington, DC: Carnegie Inst. Washington
Sandage A. 1971. In *Nuclei of Galaxies,* ed. DJK O'Connell, p. 271. Vatican City: Pontifical Acad. Sci.
Sanders DB, Soifer BT, Elias JH, Madore BF, Matthews K, Neugebauer G, Scoville NZ. 1988a. *Ap. J.* 325:74
Sanders DB, Soifer BT, Elias JH, Neugebauer G, Matthews K. 1988b. *Ap. J. Lett.* 328:L35
Sargent WLW. 1987. See Backer 1987, p. 62
Sargent WLW, Young PJ, Boksenberg A, Shortridge K, Lynds CR, Hartwick FDA. 1978. *Ap. J.* 221:731
Schechter P. 1976. *Ap. J.* 203:297
Schweizer F. 1980. *Ap. J.* 237:303
Sellgren K, Hall DNB, Kleinmann SG, Scoville NZ. 1987. *Ap. J.* 317:881
Sellgren K, McGinn MT, Becklin EE, Hall

DNB. 1990. *Ap. J.* 359:112
Sembay S, West RG. 1993. *MNRAS* 262:141
Shapiro SL. 1985. In *IAU Symp. 113, Dynamics of Star Clusters,* ed. J Goodman, P Hut, p. 373. Dordrecht: Reidel
Simien F, de Vaucouleurs G. 1986. *Ap. J.* 302:564
Small TA, Blandford RD. 1992. *MNRAS* 259:725
Soltan A. 1982. *MNRAS* 200:115
Statler TS. 1995. *Astron. J.* 109:1371
Stiavelli M, Møller P, Zeilinger WW. 1993. *Astron. Astrophys.* 277:421
Tenorio-Tagle G, Terlevich R, Franco J, Melnick J. 1992. See Filippenko 1992a, p. 147
Terlevich R. 1992. See Filippenko 1992a, p. 133
Terlevich RJ, Boyle BJ. 1993. *MNRAS* 262:491
Terlevich R, Melnick J. 1985. *MNRAS* 213:841
Terlevich R, Melnick J, Moles M. 1987. In *Observational Evidence for Activity in Galaxies,* ed. E Ye Khachikyan, KJ Fricke, J Melnick, p. 499. Dordrecht: Reidel
Terlevich R, Tenorio-Tagle G, Franco J, Melnick J, Boyle BJ. 1993. See Beckman et al 1993, p. 181
Tonry JL. 1984. *Ap. J. Lett.* 283:L27
Tonry JL. 1987. *Ap. J.* 322:632
Tremaine S. 1995. *Astron. J.* In press
Tremaine S, Ostriker JP. 1982. *Ap. J.* 256:435
Tremaine S, Richstone DO, Byun Y-I, Dressler A, Faber SM, et al. 1994. *Astron. J.* 107:634
Tully RB, Shaya EJ, Pierce MJ. 1992. *Ap. J. Suppl.* 80:479
Turner JL, Ho PTP. 1994. *Ap. J.* 421:122
van Albada GD, van der Hulst JM. 1982. *Astron. Astrophys.* 115:263
van den Bergh S. 1991. *Publ. Astron. Soc. Pac.* 103:609
van den Bosch FC, van der Marel RP. 1995. *MNRAS* In press
van der Kruit PC. 1973. *Astron. Astrophys.* 29:249
van der Kruit PC, Oort JH, Mathewson DS. 1972. *Astron. Astrophys.* 21:169
van der Marel RP. 1994a. *MNRAS* 270:271
van der Marel RP. 1994b. *Ap. J. Lett.* 432:L91
van der Marel RP. 1994c. In *Highlights of Astronomy,* Vol. 10, ed. J Bergeron. Dordrecht: Kluwer. In press
van der Marel RP, de Zeeuw T, Rix H-W, White SDM. 1995. To be published
van der Marel RP, Evans NW, Rix H-W, White SDM, de Zeeuw T. 1994b. *MNRAS* 271:99
van der Marel RP, Franx M. 1993. *Ap. J.* 407:525
van der Marel RP, Rix H-W, Carter D, Franx M, White SDM, de Zeeuw T. 1994a. *MNRAS* 268:521
Wagner SJ, Dettmar R-J, Bender R. 1989. *Astron. Astrophys.* 215:243
Walker MF. 1962. *Ap. J.* 136:695
Watson WD, Wallin BK. 1994. *Ap. J. Lett.* 432:L35
Winsall ML, Freeman KC. 1993. *Astron. Astrophys.* 268:443
Wolfe AM, Burbidge GR. 1970. *Ap. J.* 161:419
Wrobel JM, Heeschen DS. 1991. *Astron. J.* 101:148
Young PJ, Sargent WLW, Kristian J, Westphal JA. 1979. *Ap. J.* 234:76
Young PJ, Westphal JA, Kristian J, Wilson CP, Landauer FP. 1978. *Ap. J.* 221:721
Zel'dovich Ya B. 1964. *Sov. Phys. Dokl.* 9:195
Zhao J-H, Goss WM, Lo K-Y, Ekers RD. 1992. See Filippenko 1992a, p. 295